ORGANOMETALLICS
Article

Organometallics **2011,** *30,* 697–711 697
DOI: 10.1021/om100864g

Acceptor PCP Pincer Iridium(I) Chemistry: Stabilization of Nonmeridional PCP Coordination Geometries

Jeramie J. Adams, Navamoney Arulsamy, and Dean M. Roddick*

Department of Chemistry, Box 3838, University of Wyoming, Laramie, Wyoming 82071, United States

Received September 6, 2010

The preparation of a series of four-coordinate complexes $(^{CF_3}PCP)Ir(L)$ (L = CO, DBU, nbe, coe, $MeP(C_2F_5)_2$ (dfmp)) and five-coordinate complexes $(^{CF_3}PCP)Ir(L)(L')$ ($L = L'$ = CO, dfmp, nbd, cod, $(C_2F_5)_2PCH_2CH_2P(C_2F_5)_2$ (dfepe); L = PhCN, $L' = C_2H_4$) from dehydrohalogenation of $(^{CF_3}PCP)Ir(C_2H_4)(H)Cl$ with Et_3N in the presence of trapping ligands is reported. $(^{CF_3}PCP)Ir(L)$ and $(^{CF_3}PCP)Ir(L)_2$ for L = CO, dfmp have been structurally characterized and establish a distorted-trigonal -bipyramidal coordination geometry for $(^{CF_3}PCP)Ir(L)_2$ with a bent PCP unit and inequivalent axial and equatorial L coordination sites. $(^{CF_3}PCP)Ir(L)(L')$ systems ($L = L'$ = CO, C_2H_4; L = PhCN, $L' = C_2H_4$) are highly fluxional, with ligand site interconversion free energy barriers determined by VT NMR of 9.7 kcal mol^{-1} ($L = L'$ = CO), 12.2 kcal mol^{-1} ($L = L' = C_2H_4$), and 16.1 kcal mol^{-1} ($L = C_2H_4$, L' = PhCN). A dissociative site exchange mechanism is proposed. $(^{CF_3}PCP)Ir(L)$ complexes readily undergo oxidative addition reactions. Addition of H_2 to (^{CF_3}PCP)-Ir(CO) reversibly forms *trans*-$(^{CF_3}PCP)Ir(CO)(H)_2$ at ambient temperatures. In contrast, addition of H_2 to $(^{CF_3}PCP)Ir(dfmp)$ affords *fac*,*cis*-$(^{CF_3}PCP)Ir(dfmp)(H)_2$ as the major product, with an unusual facially coordinated pincer group. VT NMR monitoring of the reaction of $(^{CF_3}PCP)Ir(CO)$ with H_2 established the initial formation of *fac*,*cis*-$(^{CF_3}PCP)Ir(CO)(H)_2$ followed by conversion to *mer*,*cis*-$(^{CF_3}PCP)Ir(CO)(H)_2$ prior to isomerization to *mer*,*trans*-$(^{CF_3}PCP)Ir(CO)(H)_2$. The unusual stability of $(^{CF_3}PCP)Ir(L)_2$ and *fac*,*cis*-$(^{CF_3}PCP)Ir(L)(H)_2$ complexes is attributable to the increased stability of nonplanar (PCP)M moieties possessing strongly π-accepting phosphorus groups.

Introduction

There is continuing interest in stoichiometric and catalytic transformations mediated by pincer transition-metal complexes.[1] Of particular importance are alkane dehydrogenation and hydrogen transfer systems based on iridium phosphine pincer compounds, (PCP)Ir.[2–4] Key intermediates in alkane dehydrogenation are (PCP)Ir^{I} pincer complexes. To date, most Ir(I) pincer chemistry has focused on ^{R}PCP (R = ^{i}Pr, ^{t}Bu; PCP = $1,3\text{-}C_6H_3(CH_2P(R)_2)_2$) and resorcinol-derived ^{tBu}POCOP (POCOP = $1,3\text{-}C_6H_3(OP(R)_2)_2$) systems with strongly donating phosphorus substituents.[2d,g,5] It is significant that less electron-rich ^{tBu}POCOP pincer catalysts are ~10 times more active than ^{R}PCP analogues and involve different preferences for catalyst resting states.[2g,6] In light of these observations, expanding the range of pincer systems, particularly electron-poor complexes of Ir(I), is clearly of interest.

In our previous paper we presented the synthesis and characterization of Ir(III) pincer systems with the strongly π-accepting CF_3-substituted ligand ^{CF_3}PCP.[7] A general property noted in this chemistry was the enhanced Lewis

---

(1) (a) Albrecht, M.; van Koten, G. *Angew. Chem., Int. Ed.* **2001**, *40*, 3750–3781. (b) Singleton, J. T. *Tetrahedron* **2003**, *59*, 1837–1857. (c) van der Boom, M. E.; Milstein, D. *Chem. Rev.* **2003**, *103*, 1759–1792. (d) Morales-Morales, D. J., Craig, M *The Chemistry of Pincer Compounds*; Elsevier: Amsterdam, 2007. (e) Benito-Garagorri, D.; Kirchner, K. *Acc. Chem. Res.* **2008**, *41*, 201–213. (f) Morales-Morales, D. *Mini-Rev. Org. Chem.* **2008**, *5*, 141–152.

(2) (a) Gupta, M.; Hagen, C.; Flesher, R. J.; Kaska, W. C.; Jensen, C. M. *Chem. Commun.* **1996**, 2083–2084. (b) Xu, W.-w.; Rosini, G. P.; Krogh-Jespersen, K.; Goldman, A. S.; Gupta, M.; Jensen, C. M.; Kaska, W. C. *Chem. Commun.* **1997**, 2273–2274. (c) Jensen, C. M. *Chem. Commun.* **1999**, 2443–2449. (d) Liu, F.; Goldman, A. S. *Chem. Commun.* **1999**, 655–656. (e) Liu, F.; Pak, E. B.; Singh, B.; Jensen, C. M.; Goldman, A. S. *J. Am. Chem. Soc.* **1999**, *121*, 4086–4087. (f) Kanzelberger, M.; Singh, B.; Czerw, M.; Krogh-Jespersen, K.; Goldman, A. S. *J. Am. Chem. Soc.* **2000**, *122*, 11017–11018. (g) Goettker-Schnetmann, I.; White, P.; Brookhart, M. *J. Am. Chem. Soc.* **2004**, *126*, 1804–1811. (h) Ray, A.; Zhu, K.; Kissin, Y. V.; Cherian, A. E.; Coates, G. W.; Goldman, A. S. *Chem. Commun.* **2005**, 3388–3390. (i) Kuklin, S. A.; Sheloumov, A. M.; Dolgushin, F. M.; Ezernitskaya, M. G.; Peregudov, A. S.; Petrovskii, P. V.; Koridze, A. A. *Organometallics* **2006**, *25*, 5466–5476.

(3) (a) Goldman, A. S.; Roy, A. H.; Huang, Z.; Ahuja, R.; Schinski, W.; Brookhart, M. *Science (Washington, DC, U.S.)* **2006**, *312*, 257–261. (b) Ahuja, R.; Kundu, S.; Goldman, A. S.; Brookhart, M.; Vicente, B. C.; Scott, S. L. *Chem. Commun.* **2008**, 253–255. (c) Bailey, B. C.; Schrock, R. R.; Kundu, S.; Goldman, A. S.; Huang, Z.; Brookhart, M. *Organometallics* **2009**, *28*, 355–360.

(4) (a) Goldman, A. S.; Brookhart, M.; Huang, Z.; Krogh-Jespersen, K.; Kundu, S.; Scott, S. L. *Prepr. Symp.-Am. Chem. Soc., Div. Fuel Chem.* **2009**, *54*, 213–215. (b) Huang, Z.; Brookhart, M.; Goldman, A. S.; Kundu, S.; Ray, A.; Scott, S. L.; Vicente, B. C. *Adv. Synth. Catal.* **2009**, *351*, 188–206. (c) Huang, Z.; Rolfe, E.; Carson, E. C.; Brookhart, M.; Goldman, A. S.; El-Khalafy, S. H.; MacArthur, A. H. R. *Adv. Synth. Catal.* **2010**, *352*, 125–135.

(5) Kundu, S.; Choliy, Y.; Zhuo, G.; Ahuja, R.; Emge, T. J.; Warmuth, R.; Brookhart, M.; Krogh-Jespersen, K.; Goldman, A. S. *Organometallics* **2009**, *28*, 5432–5444.

(6) Goettker-Schnetmann, I.; Brookhart, M. *J. Am. Chem. Soc.* **2004**, *126*, 9330–9338.

acidity and binding of 16-electron $(^{CF_3}PCP)Ir(X)(Y)$ centers to form coordinatively saturated octahedral $(^{CF_3}PCP)Ir(X)(Y)(L)$ products. In this paper we report the synthesis of a number of four-coordinate $(^{CF_3}PCP)Ir(L)$ as well as five-coordinate $(^{CF_3}PCP)Ir(L)_2$ products. $(^{CF_3}PCP)Ir(L)_2$ compounds have a distorted-trigonal-bipyramidal geometry with inequivalent L binding sites. $(^{CF_3}PCP)Ir(L)$ (L = CO, $MeP(C_2F_5)_2$ (dfmp)) complexes react readily with H_2 to produce $(^{CF_3}PCP)Ir(L)(H)_2$ products. The unique ability of acceptor PCP ligands to undergo a nonplanar distortion in five-coordinate systems is extended further to the characterization of unprecedented facial octahedral products, *fac*, *cis*-$(^{CF_3}PCP)Ir(L)(H)_2$ (L = CO, dfmp).

Results and Discussion

Dehydrohalogenation Chemistry of $(^{CF_3}PCP)Ir(L)(H)Cl$ (L = CO, C_2H_4, MeCN, PhCN, $MeP(C_2F_5)_2$) in the Absence of a Trapping Ligand. Dehydrohalogenation of $(^{CF_3}PCP)Ir(L)(H)Cl$ systems (L = CO, C_2H_4, MeCN, PhCN, $MeP(C_2F_5)_2$) using reagents such as KO^tBu, $LiEt_3BH$, and KH, which are commonly employed with donor systems $(^{R}PCP)Ir(H)Cl$, failed to produce either $(^{CF_3}PCP)Ir(L)$ or $(^{CF_3}PCP)Ir(L)(H)_2$ products in the presence of H_2. Complex product mixtures were observed when L was CO or MeCN. Previous studies with $(^{CF_3}PCP)PtCl$, using the basic reagent KH, suggested that the benzylic hydrogens of ^{CF_3}PCP are susceptible to deprotonation,[8] and similar pincer arm deprotonation chemistry has been reported in related systems.[9] The milder base Et_3N does, however, readily dehydrohalogenate $(^{CF_3}PCP)Ir(CO)(H)Cl$ in benzene to cleanly afford $(^{CF_3}PCP)Ir(CO)$ (**1**) (eq 1). Benzylic proton resonances for complex **1** are replaced by a single multiplet at δ 3.29, indicating lateral symmetry across the plane defined by the meridional (PCP)Ir unit. ^{19}F NMR spectra similarly show a single multiplet at −57.5 ppm.

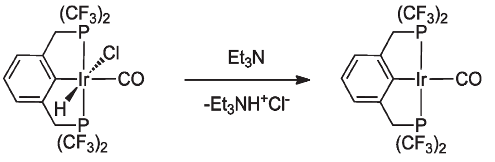

1

(1)

The carbonyl IR stretching frequency for **1**, 2018 cm^{-1}, is 105 cm^{-1} greater than the ν(CO) frequency reported for $(^{tBu}PCP)Ir(CO)$, demonstrating a significant decrease in CO−metal π back-bonding. The resorcinol pincer derivatives (R-^{tBu}POCOP)Ir(CO) (R = MeO, Me, H, F, C_6F_5, *m*-$\{(C_6H_3)(CF_3)_2\}$) are more electron rich and have carbonyl stretching frequencies ranging between 1947 and 1955 cm^{-1}.[10]

Attempts to dehydrohalogenate more electron rich (and presumably less acidic) $(^{CF_3}PCP)Ir(L)(H)Cl$ complexes (L = MeCN, PhCN) with Et_3N in the absence of trapping ligands were not successful. In the case of the acceptor phosphine complex $(^{CF_3}PCP)Ir(dfmp)(H)Cl$ (dfmp = $MeP(C_2F_5)_2$), partial reaction was observed (ca. 10% after 72 h). DBU (1,5-diazabicyclo[4.3.0]non-5-ene) has recently been employed for (PCP)Ir(CO)(H)Cl dehydrochlorination[11] and was examined for $(^{CF_3}PCP)Ir(L)(H)Cl$ systems. Reaction of $(^{CF_3}PCP)Ir(MeCN)(H)Cl$ with DBU afforded not $(^{CF_3}PCP)Ir(MeCN)$ but rather a red product identified as the DBU adduct $(^{CF_3}PCP)Ir(DBU)$ (**2**) (eq 2). Reaction of the Ir(III) acetonitrile complex with 1 equiv of DBU in benzene at ambient temperature gave a 1:1 mixture of unreacted starting material and **2**. The loss of lateral symmetry due to the perpendicular orientation of the bicyclic DBU ligand relative to the (PCP)Ir unit was indicated by diastereotopic benzylic protons at 3.46 and 3.30 ppm and inequivalent CF_3 groups at −60.2 and −60.6 ppm and was confirmed by X-ray diffraction (Figure 1). Structurally characterized transition-metal DBU adducts are rare.[12]

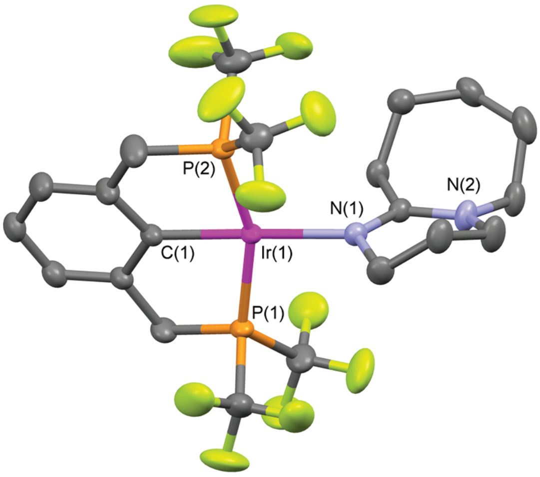

Figure 1. Molecular structure of $(^{CF_3}PCP)Ir(DBU)$ (**2**) with 50% probability thermal ellipsoids and hydrogen atoms omitted for clarity. Selected bond distances (Å) and angles (deg): Ir(1)−C(1) = 2.047(4), Ir(1)−N(1) = 2.135(3), Ir(1)−P(1) = 2.1889(9), Ir(1)−P(2) = 2.1892(9); C(1)−Ir(1)−N(1) = 178.14(13), C(1)−Ir(1)−P(1) = 80.02(10), N(1)−Ir(1)−P(1) = 98.44(9), C(1)−Ir(1)−P(2) = 80.43(10), N(1)−Ir(1)−P(2) = 101.26(9), P(1)−Ir(1)−P(2) = 158.27(4).

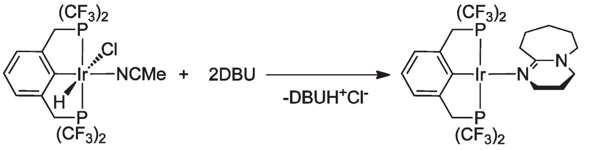

2

(2)

$(^{CF_3}PCP)Ir(CO)$ Reactivity with CO. Five-coordinate Ir(I) complexes of the general types $(R_3P)_x(CO)_{4-x}Ir(Y)$ (Y = H, halide, hydrocarbyl) and $(R_3P)_x(CO)_{5-x}Ir^+$ are fairly common,[13,14] but corresponding pincer complexes have not been well established. Milstein has reported that electron-poor pyrollyl-substituted rhodium pincer phosphine complexes $(^{pyr}PCP)Rh(PR_3)$ (R = Et, Ph, Pyr) readily add CO to form $(^{pyr}PCP)Rh(PEt_3)(CO)$ and predicted on the basis of DFT calculations that ^{R}PCP ligands with stronger

---

[7] Adams, J. J.; Arulsamy, N.; Roddick, D. M. *Organometallics* **2011**, *30*, DOI 10.1021/om1008633.

[8] Adams, J. J.; Arulsamy, N.; Roddick, D. M. *Organometallics* **2009**, *28*, 1148–1157.

[9] Ben-Ari, E.; Leitus, G.; Shimon, L. J. W.; Milstein, D. *J. Am. Chem. Soc.* **2006**, *128*, 15390–15391.

[10] Goettker-Schnetmann, I.; White, P. S.; Brookhart, M. *Organometallics* **2004**, *23*, 1766–1776.

[11] Winter, A. M.; Eichele, K.; Mack, H.-G.; Kaska, W. C.; Mayer, H. A. *Dalton Trans.* **2008**, 527–532.

[12] (a) Bruce, M. I.; Low, P. J.; Skelton, B. W.; White, A. H. *J. Organomet. Chem.* **1996**, *515*, 65–79. (b) Barkley, J. V.; Davies, C. J.; Heaton, B. T.; Jacob, C. *J. Chem. Soc., Dalton Trans.* **1995**, 2861–2863. (c) Floerke, U.; Ortmann, U.; Haupt, H. J. *Acta Crystallogr., Sect. C* **1992**, *C48*, 1663–1665.

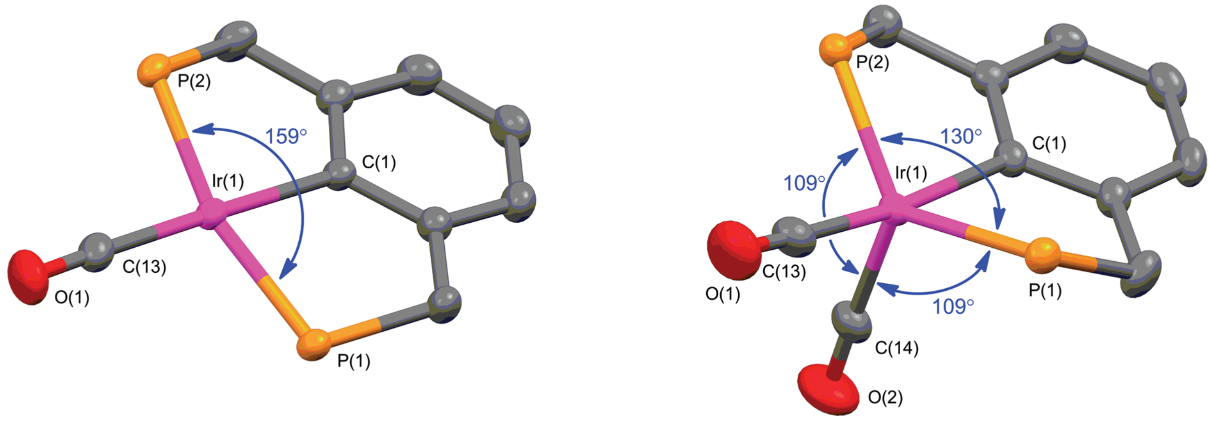

Figure 2. Molecular structures of ($^{\mathrm{CF_3}}$PCP)Ir(CO) (**1**) and ($^{\mathrm{CF_3}}$PCP)Ir(CO)$_2$ (**3**) with 50% probability thermal ellipsoids. Hydrogen atoms and CF$_3$ groups are omitted for clarity. Selected bond distances (Å) and angles (deg) for **1**: Ir(1)−C(13) = 1.895(2), Ir(1)−C(1) = 2.0876(19), Ir(1)−P(2) = 2.2198(4), Ir(1)−P(1), 2.2273(4); C(13)−Ir(1)−C(1) = 179.06(8), C(13)−Ir(1)−P(2) = 100.15(6), C(1)−Ir(1)−P(2) = 79.59(5), C(13)−Ir(1)−P(1) = 100.44(6), C(1)−Ir(1)−P(1) = 79.85(5), P(2)−Ir(1)−P(1) = 159.340(19). Selected bond distances (Å) and angles (deg) for **3**: Ir(1)−C(13) = 1.939(4), Ir(1)−C(14) = 1.941(4), Ir(1)−C(1) = 2.131(3), Ir(1)−P(2) = 2.2435(8), Ir(1)−P(1) = 2.2509(8); C(13)−Ir(1)−C(14) = 96.71(15), C(13)−Ir(1)−C(1) = 171.64(13), C(14)−Ir(1)−C(1) = 91.56(13), C(13)−Ir(1)−P(2) = 97.65(11), C(14)−Ir(1)−P(2) = 114.35(11), C(1)−Ir(1)−P(2) = 77.76(9), C(13)−Ir(1)−P(1) = 99.71(11), C(14)−Ir(1)−P(1) = 109.37(11), C(1)−Ir(1)−P(1) = 78.53(8), P(2)−Ir(1)−P(1) = 130.26(3).

π-accepting abilities should favor the formation of the dicarbonyl ($^{\mathrm{R}}$PCP)M(CO)$_2$.[15] In accord with this expectation, addition of 1 atm of CO to an orange benzene solution of **1** at ambient temperature resulted in a rapid irreversible reaction to give a colorless solution of the dicarbonyl ($^{\mathrm{CF_3}}$PCP)Ir(CO)$_2$ (**3**) (eq 3). Complex **3** was also prepared directly from ($^{\mathrm{CF_3}}$PCP)Ir(CO)(H)Cl and Et$_3$N in the presence of 1 atm of CO in good yield. ν(CO) bands for **3** appear at 2068 and 2020 cm^{-1}. Both **1** and **3** have been crystallographically characterized (Figure 2)

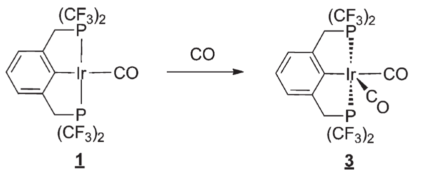

(3)

Dehydrohalogenation Chemistry of ($^{\mathrm{CF_3}}$PCP)Ir(L)(H)Cl in the Presence of Monodentate and Bidentate Trapping Ligands. The reaction of ($^{\mathrm{CF_3}}$PCP)Ir(C$_2$H$_4$)(H)Cl with Et$_3$N in the presence of 1 atm of C$_2$H$_4$ at ambient temperature generates a product identified by NMR as the bis-ethylene adduct ($^{\mathrm{CF_3}}$PCP)Ir(C$_2$H$_4$)$_2$ (**4**). The presence of two ethylene ligands was indicated by ambient-temperature ^{1}H NMR spectra, which show a broadened ($\nu_{1/2}$ = 120 Hz) C$_2$H$_4$ resonance at δ 2.38 integrating to 2/1 with respect to the benzylic resonance at δ 3.22. While **4** could be isolated as a white solid by cold filtration from hexane in under 1 atm of C$_2$H$_4$, removal of the volatiles resulted in partial ethylene loss and formation of an impure oily red-orange product. The ethylene loss product was not identified. Placing a benzene solution of impure **4** under 1 atm of ethylene regenerated a colorless solution and resulted in a sharpening of the ^{31}P pincer broad resonance into a well-defined multiplet at 48.5 ppm. Under 1 atm of ethylene, the coordinated ethylene proton resonance of **4** broadened further ($\nu_{1/2} \approx$ 160 Hz) and a very broad ($\nu_{1/2} \approx$ 300 Hz) free ethylene resonance was observed at δ 5.15 in a 2/0.5 ratio, which indicated facile intermolecular ethylene exchange on the NMR time scale at ambient temperature (see below).

Despite the relatively intractable nature of ($^{\mathrm{CF_3}}$PCP)Ir(C$_2$H$_4$), in situ prepared ($^{\mathrm{CF_3}}$PCP)Ir(C$_2$H$_4$)$_2$ serves as a useful precursor to many ($^{\mathrm{CF_3}}$PCP)Ir(L)$_x$ systems (Scheme 1). Indeed, the addition of ethylene as a coreagent in dehydrohalogenation reactions is often essential for efficient syntheses. For instance, dehydrohalogenation of ($^{\mathrm{CF_3}}$PCP)Ir(C$_2$H$_4$)(H)Cl with Et$_3$N in the presence of 1−4 equiv of dfmp in the presence of C$_2$H$_4$ afforded orange ($^{\mathrm{CF_3}}$PCP)Ir(dfmp) (**5**) in high yield. Two ^{31}P resonances are observed at 67.3 and 37.1 ppm in a 2/1 ratio and are assigned to the $^{\mathrm{CF_3}}$PCP and dfmp ligands, respectively. **5** has moderate air stability as a solid and may be stored indefinitely under an inert atmosphere. Addition of excess dfmp (10+ equiv) to **5** in benzene resulted in the precipitation of colorless crystalline ($^{\mathrm{CF_3}}$PCP)Ir(dfmp)$_2$ (**6**). Attempts to isolate **6** on a preparative scale resulted in mixtures of **5** and **6** due to facile dfmp loss under vacuum. Both **5** and **6** were characterized by X-ray diffraction (Figure 3).

Cyclic alkene complexes ($^{\mathrm{CF_3}}$PCP)Ir(L) (L = norbornene, cyclooctene) were obtained from ($^{\mathrm{CF_3}}$PCP)Ir(C$_2$H$_4$)(H)Cl

---

(13) (a) Payne, N. C.; Ibers, J. A. *Inorg. Chem.* **1969**, *8*, 2714–2718. (b) Ciechanowicz, M.; Skapski, A. C.; Troughton, P. G. H. *Acta Crystallogr., Sect. B* **1976**, *B32*, 1673–1680. (c) Dahlenburg, L.; Mirzaei, F. *J. Organomet. Chem.* **1983**, *251*, 123–132. (d) Churchill, M. R.; Fettinger, J. C.; Rees, W. M.; Atwood, J. D. *J. Organomet. Chem.* **1986**, *304*, 227–238. (e) Lilga, M. A.; Sohn, Y. S.; Ibers, J. A. *Organometallics* **1986**, *5*, 766–771. (f) Deutsch, P. P.; Eisenberg, R. *Organometallics* **1990**, *9*, 709–718. (g) Abu-Hasanayn, F.; Emge, T. J.; Maguire, J. A.; Krogh-Jespersen, K.; Goldman, A. S. *Organometallics* **1994**, *13*, 5177–5180. (h) Casey, C. P.; Paulsen, E. L.; Beuttenmueller, E. W.; Proft, B. R.; Matter, B. A.; Powell, D. R. *J. Am. Chem. Soc.* **1999**, *121*, 63–70. (i) Fox, D. J.; Duckett, S. B.; Flaschenriem, C.; Brennessel, W. W.; Schneider, J.; Gunay, A.; Eisenberg, R. *Inorg. Chem.* **2006**, *45*, 7197–7209.

(14) (a) Mague, J. T.; Lloyd, C. L. *Organometallics* **1988**, *7*, 983–993. (b) Balch, A. L.; Catalano, V. J.; Noll, B. C.; Olmstead, M. M. *J. Am. Chem. Soc.* **1990**, *112*, 7558–7566. (c) Balch, A. L.; Catalano, V. J.; Olmstead, M. M. *J. Am. Chem. Soc.* **1990**, *112*, 2010–2011. (d) Randall, S. L.; Thompson, J. S.; Buttrey, L. A.; Ziller, J. W.; Churchill, M. R.; Atwood, J. D. *Organometallics* **1991**, *10*, 683–688. (e) Randall, S. L.; Miller, C. A.; See, R. F.; Churchill, M. R.; Janik, T. S.; Lake, C. H.; Atwood, J. D. *Organometallics* **1994**, *13*, 5088–5095.

(15) Kossoy, E.; Iron Mark, A.; Rybtchinski, B.; Ben-David, Y.; Shimon Linda, J. W.; Konstantinovski, L.; Martin Jan, M. L.; Milstein, D. *Chemistry* **2005**, *11*, 2319–2326.

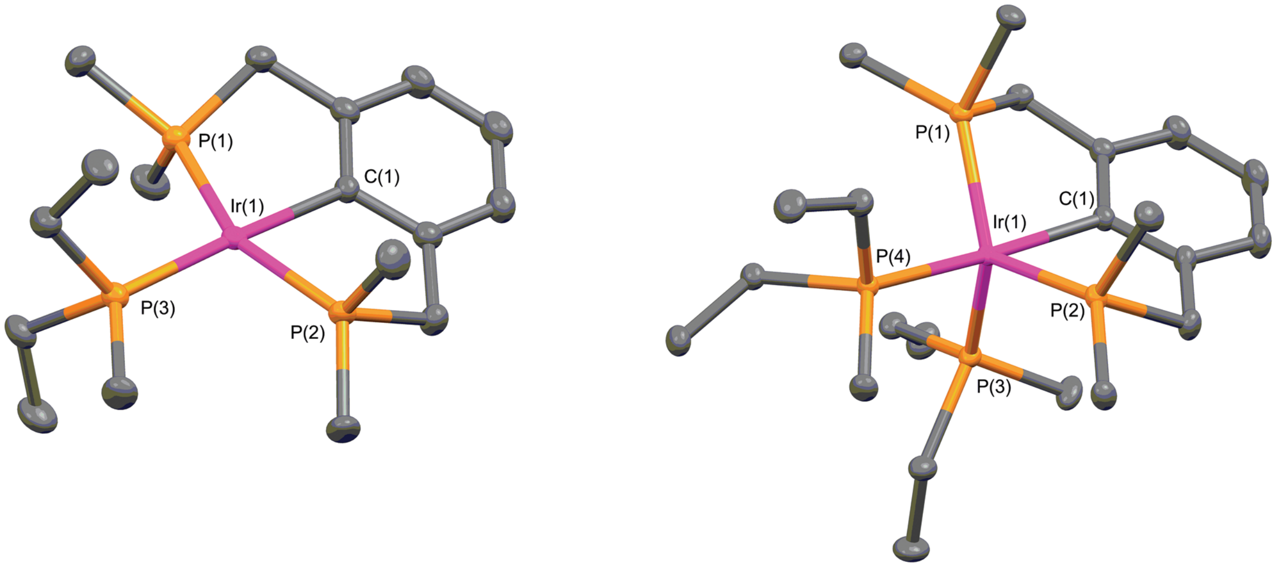

Figure 3. Molecular structures of (^{CF_3}PCP)Ir(dfmp) (**5**) and (^{CF_3}PCP)Ir(dfmp)$_2$ (**6**) with 50% probability thermal ellipsoids. Hydrogen and fluorine atoms are omitted for clarity. Selected bond distances (Å) and angles (deg) for **5**: Ir(1)−C(1) = 2.118(3), Ir(1)−P(2) = 2.2280(10), Ir(1)−P(1) = 2.2455(10), Ir(1)−P(3) = 2.2546(10); C(1)−Ir(1)−P(2) = 77.90(11), C(1)−Ir(1)−P(1) = 77.57(11), P(2)−Ir(1)−P(1) = 155.46(4), C(1)−Ir(1)−P(3) = 177.31(11), P(2)−Ir(1)−P(3) = 101.15(4), P(1)−Ir(1)−P(3) = 103.39(4). Selected bond distances (Å) and angles (deg) for **6**: Ir(1)−C(1) = 2.1377(16), Ir(1)−P(2) = 2.2602(4), Ir(1)−P(1) = 2.2668(4), Ir(1)−P(3) = 2.3089(4), Ir(1)−P(4) = 2.3120(4); C(1)−Ir(1)−P(2) = 77.16(5), C(1)−Ir(1)−P(1) = 76.54(5), P(2)−Ir(1)−P(1) = 124.211(16), C(1)−Ir(1)−P(3) = 84.38(5), P(2)−Ir(1)−P(3) = 110.827(16), P(1)−Ir(1)−P(3) = 114.397(16), C(1)−Ir(1)−P(4) = 173.59(5), P(2)−Ir(1)−P(4) = 98.998(16), P(1)−Ir(1)−P(4) = 101.900(15), P(3)−Ir(1)−P(4) = 101.854(15).

Scheme 1

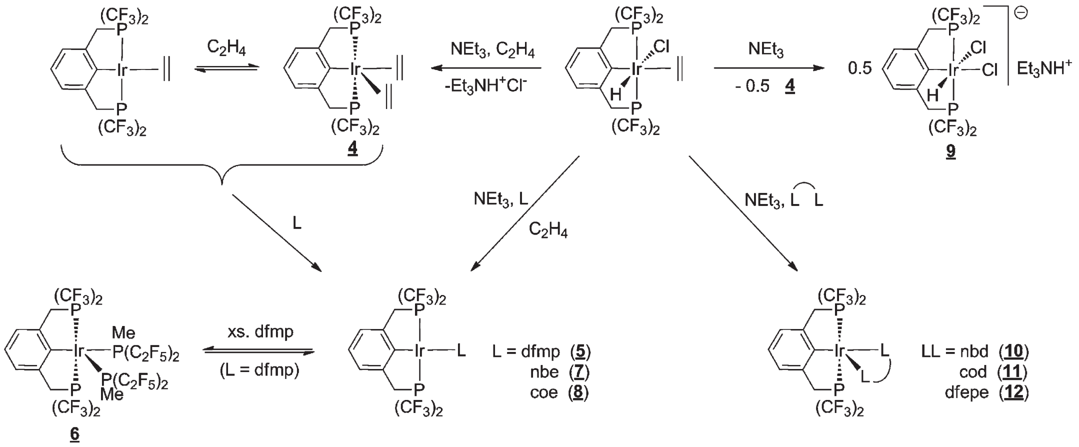

and Et$_3$N in the presence of 1 atm of C$_2$H$_4$ and excess olefin. Monitoring the solution by NMR after the precipitation of Et$_3$NH$^+$Cl$^-$ showed the bis-ethylene complex **4** to be the only observed iridium species; filtration and concentration resulted in loss of ethylene and conversion to (^{CF_3}PCP)-Ir(nbe) (**7**) or (^{CF_3}PCP)Ir(coe) (**8**). ^{1}H NMR data for **7** and **8** are consistent with alkene coordination: phosphorus-coupled vinylic norbornene protons ($^3J_{PH}$ = 5 Hz) in **7** appear as a triplet at δ 4.11, a singlet bridgehead resonance occurs at δ 3.11, and four separate resonances are observed for the diastereotopic nbe methylene protons. Vinylic coe protons for **8** appear as a broad unresolved resonance at δ 5.03, and coe methylene protons are observed between δ 2.53 and 1.27. While norbornene NMR data are consistent with the solid-state structure shown in Figure 4, single PCP benzylic and CF$_3$ resonances indicate that alkene rotation is rapid on the NMR time scale at ambient temperature. NMR data for **8** are similar to those for **7**. Unlike the sharp CF$_3$ multiplet observed for **7**, however, the CF$_3$ resonance for **8** is significantly broadened and suggests that slower CF$_3$ site exchange is occurring on the NMR time scale for the coe adduct.

The presence of ethylene in the synthesis of **7** and **8** is critical: dehydrohalogenation of (^{CF_3}PCP)Ir(C$_2$H$_4$)(H)Cl with excess nbe or coe in the absence of added C$_2$H$_4$ resulted in partial dehydrohalogenation (~50%) after 20 h and the formation of the side product (^{CF_3}PCP)Ir(H)Cl$_2^-$HNEt$_3^+$ (**9**). X-ray diffraction (see the Supporting Information) and NMR spectroscopy confirmed the formulation of **9**. In the absence of any added trapping ligand, the addition of Et$_3$N to (^{CF_3}PCP)Ir(C$_2$H$_4$)(H)Cl in benzene produces a 1/1 mixture of **9** and the bis-ethylene adduct **4**. Complex **9** is presumably derived from the reaction of chloride (either as free Cl^- or as an associated chloride adduct such as $(^{CF_3}PCP)Ir(C_2H_4)Cl^-$) with unreacted $(^{CF_3}PCP)Ir(C_2H_4)(H)Cl$. This is supported by a separate NMR experiment: agitating a 1:1 mixture of $(^{CF_3}PCP)Ir(C_2H_4)(H)Cl$ and $HNEt_3^+Cl^-$ in benzene at 20 °C resulted in the quantitative formation of **9** after 20 min. Monitoring the reaction of $(^{CF_3}PCP)Ir(C_2H_4)(H)Cl$ with Et_3N by NMR under 1 atm of C_2H_4 showed that **9** was present after 8 h (~50%), but after 24 h it was cleanly converted to the bis-ethylene complex **4**.

Dehydrohalogenation chemistry with the chelating trapping ligands norbornadiene, 1,5-cyclooctadiene, and $(C_2F_5)_2PCH_2CH_2P(C_2F_5)_2$ (dfepe) cleanly affords $(^{CF_3}PCP)Ir(LL)$ products (LL = nbd (**10**), cod (**11**), dfepe (**12**)) in high yields. Complexes **11** and **12** were structurally characterized (Figure 5). For these chelates, the addition of ethylene as a coreactant is not required. Designing highly electrophilic metal systems using perfluoroalkylphosphines (PFAP's) has been a longstanding interest of our research group. In this context, the dfepe complex **12** is similar to the five-coordinate Ir(I) complex $(dfepe)_2IrH$, reported previously by our group.[16]

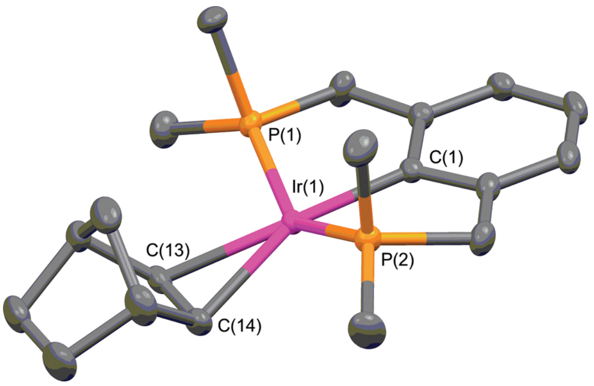

Figure 4. Molecular structure of $(^{CF_3}PCP)Ir(nbe)$ (**7**) with 50% probability thermal ellipsoids. Hydrogen and fluorine atoms are omitted for clarity. Selected bond distances (Å) and angles (deg) for **7**: Ir(1)−C(1) = 2.089(2), Ir(1)−P(2) = 2.1930(6), Ir(1)−P(1) = 2.1995(6), Ir(1)−C(13) = 2.264(2), Ir(1)−C(14) = 2.270(2); C(1)−Ir(1)−P(2) = 78.53(6), C(1)−Ir(1)−P(1) = 79.38(6), P(2)−Ir(1)−P(1) = 142.30(2).

Dehydrohalogenation of nitrile adducts $(^{CF_3}PCP)Ir(RCN)(H)Cl$ with Et_3N in the presence of excess MeCN or PhCN does not afford $(^{CF_3}PCP)Ir(nitrile)_x$ products. Instead, dehydrohalogenation of $(^{CF_3}PCP)Ir(PhCN)(H)Cl$ in the presence of excess C_2H_4 and PhCN gave the mixed five-coordinate complex $(^{CF_3}PCP)Ir(PhCN)(C_2H_4)$ (**13**) (eq 4). As with other five-coordinate $(^{CF_3}PCP)Ir$ systems, the loss of lateral symmetry across the (PCP)Ir unit is reflected by distinct ^{19}F CF_3 doublets at δ −56.8 and −62.3 and diastereotopic benzylic proton resonances at δ 3.52 and 3.37. An interesting feature of the ^1H NMR spectrum is the appearance of two broadened singlet C_2H_4 resonances at δ 2.60 and 1.76, which may reflect either geminal or vicinal chemical inequivalence, depending on the orientation of the ethylene ligand. This issue was resolved by ^{13}C NMR and X-ray diffraction (Figure 6), which revealed that the coordinated ethylene is above the (PCP)Ir plane and is aligned parallel to the P−Ir−P plane. Thus, the two resonances are due to vicinal proton sets directed toward the PhCN and PCP aryl groups. ^{13}C NMR data for the bound ethylene ligand show an upfield single carbon resonance at 32.4 ppm with $^1J_{CH}$ = 157 Hz. This coupling is slightly lower than the $^1J_{CH}$ value reported for $(^{CF_3}PCP)Ir^{III}$ ethylene complexes[7] and is consistent with a greater degree of π back-bonding from the $(^{CF_3}PCP)Ir^I$ moiety.

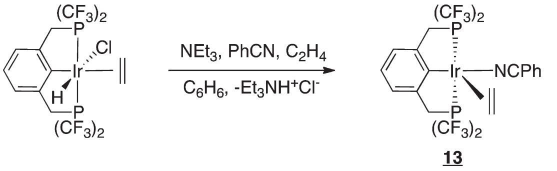

(4)

$(^{CF_3}PCP)Ir(L)_2$ Dynamics. The fluxionality of five-coordinate $(^{CF_3}PCP)Ir(L)_2$ systems has been examined by variable-temperature ^1H and ^{19}F NMR. While the solid-state structure of the dicarbonyl complex **3** shows inequivalent CO

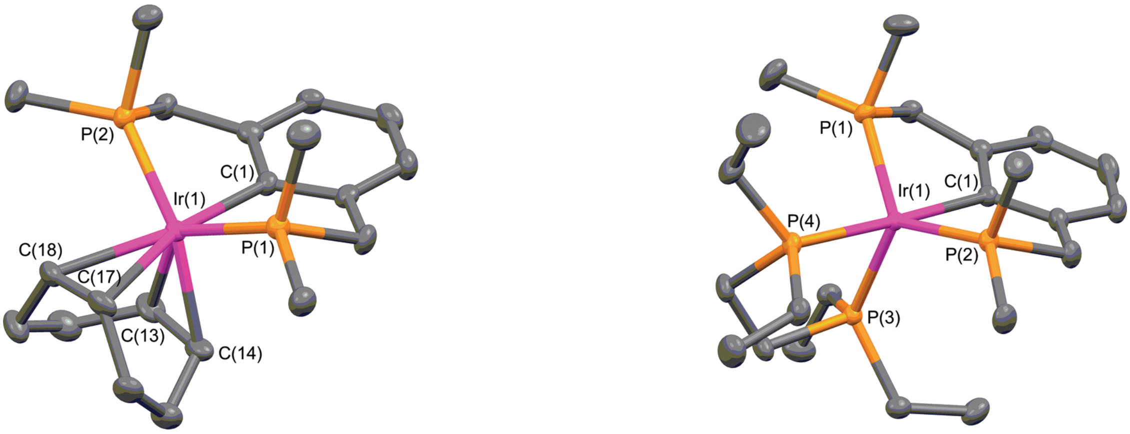

Figure 5. Molecular structures of $(^{CF_3}PCP)Ir(cod)$ (**11**) and $(^{CF_3}PCP)Ir(dfepe)$ (**12**) with 50% probability thermal ellipsoids. Hydrogen and fluorine atoms are omitted for clarity. Selected bond distances (Å) and angles (deg) for **11**: Ir(1)−C(1) = 2.097(4), Ir(1)−C(13) = 2.162(4), Ir(1)−C(14) = 2.175(4), Ir(1)−P(2) = 2.2479(11), Ir(1)−P(1) = 2.2744(11), Ir(1)−C(17) = 2.295(4), Ir(1)−C(18) = 2.299(4); C(1)−Ir(1)−P(2) = 76.80(12), C(1)−Ir(1)−P(1) = 77.50(12), P(2)−Ir(1)−P(1) = 119.02(4). Selected bond distances (Å) and angles (deg) for **12**: Ir(1)−C(1) = 2.146(2), Ir(1)−P(2) = 2.2634(6), Ir(1)−P(1) = 2.2751(6), Ir(1)−P(3) = 2.2878(5), Ir(1)−P(4) = 2.2998(6); C(1)−Ir(1)−P(2) = 77.84(6), C(1)−Ir(1)−P(1) = 76.15(6), P(2)−Ir(1)−P(1) = 126.23(2), C(1)−Ir(1)−P(3) = 96.36(6), P(2)−Ir(1)−P(3) = 119.39(2), P(1)−Ir(1)−P(3) = 109.66(2), C(1)−Ir(1)−P(4) = 177.05(6). P(2)−Ir(1)−P(4) = 104.94(2), P(1)−Ir(1)−P(4) = 101.23(2), P(3)−Ir(1)−P(4) = 83.19(2).

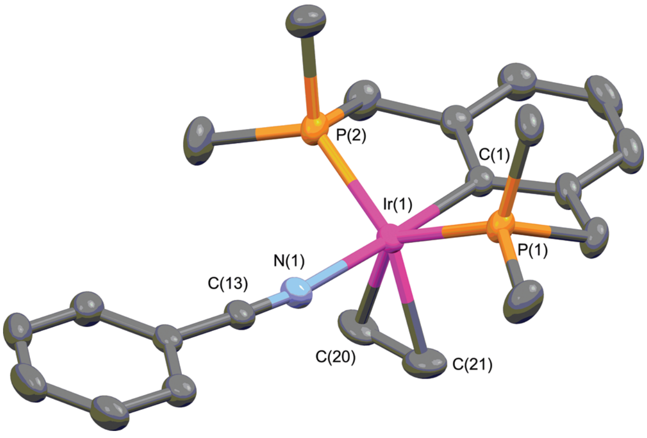

Figure 6. Molecular structure of $(^{CF_3}PCP)Ir(PhCN)(C_2H_4)$ (**13**) with 50% thermal ellipsoids. Hydrogen and fluorine atoms are omitted for clarity. Selected bond distances (Å) and angles (deg) for **13**: Ir(1)−C(1) = 2.057(4), Ir(1)−N(1) = 2.088(3), Ir(1)−C(20) = 2.174(4), Ir(1)−C(21) = 2.180(4), C(20)−C(21) = 1.412(7), Ir(1)−P(2) = 2.2185(10), Ir(1)−P(1) = 2.2243(10); C(1)−Ir(1)−N(1) = 177.88(14), C(1)−Ir(1)−P(2) = 80.30(11), N(1)−Ir(1)−P(2) = 97.58(10), C(1)−Ir(1)−P(1) = 78.59(10), N(1)−Ir(1)−P(1) = 102.71(9), P(2)−Ir(1)−P(1) = 123.78(4).

ligands disposed cis and trans to the Ir−C(aryl) bond (Figure 2), at ambient temperatures single resonances are observed for the diastereotopic pincer benzylic methylene protons and CF_3 groups in ^1H and ^{19}F NMR spectra, respectively, which indicate that CO site exchange is fast on the NMR time scale. VT NMR experiments have confirmed this: when $(^{CF_3}PCP)Ir(CO)_2$ in CD_2Cl_2 is cooled under N_2 to −95 °C, a slow-exchange limit is observed with two distinct benzylic proton resonances at δ 4.20 and δ 3.86 and well-defined CF_3 doublets at −61.4 ($^2J_{PF}$ = 75 Hz) and −65.4 ($^2J_{PF}$ = 72 Hz). Coalescence of the inequivalent benzylic groups at −70 °C and CF_3 groups at −50 °C corresponds to a site exchange activation barrier of 9.7(2) kcal mol^{-1}.

The presence of a single ethylene proton resonance for the bis-ethylene complex $(^{CF_3}PCP)Ir(C_2H_4)_2$ (**4**) at 20 °C indicates that **4** is also fluxional. VT NMR data for **4** in the absence of free ethylene show dynamic exchange processes involving both ethylene ligand rotation and ligation site equilibration (Figure 7).

At −90 °C, separate benzylic CH_2 resonances appear at δ 3.89 and 3.67, and three distinct ethylene proton resonances appear at δ 2.95, 2.70, and 1.73 in a 2/4/2 integrated ratio. ^{13}C NMR spectra at this temperature revealed two ethylene carbon resonances at 45.1 ($^1J_{CH}$ = 163 Hz) and 35.6 ($^1J_{CH}$ = 160 Hz) ppm. The presence of two, rather than three, ethylene carbon resonances indicates that the δ 2.95 and 1.73 doublets are due to inequivalent geminal, rather than vicinal, protons, and therefore the associated C_2H_4 ligand has an effective plane of symmetry relating the CH_2 groups. At temperatures above −90 °C all ethylene and benzylic resonances undergo exchange broadening. The δ 2.95 and 1.73 ethylene resonances coalesce at −10 °C, corresponding to a rotational exchange barrier of $\Delta G^{\ddagger}$ = 11.7(2) kcal mol^{-1}. At 20 °C, all ethylene resonances collapse into a single broadened resonance, and further warming to 50 °C results in progressive sharpening to an averaged ethylene signal at 2.68 ppm. A coalescence at −18 °C ($\Delta G^{\ddagger}$ = 12.2(2) kcal mol^{-1}) is observed for the diastereotopic benzylic protons. Additional dynamic information is provided by ^{19}F spectra, which show distinct CF_3 resonances at −58.7 and −65.3 ppm at −90 °C and a coalescence temperature of +30 °C, corresponding to a slightly higher $\Delta G^{\ddagger}$ value of 12.6(2) kcal mol^{-1}. These observations are consistent with similar exchange barriers for the rotation of one ethylene ligand and ethylene ligand site exchange.

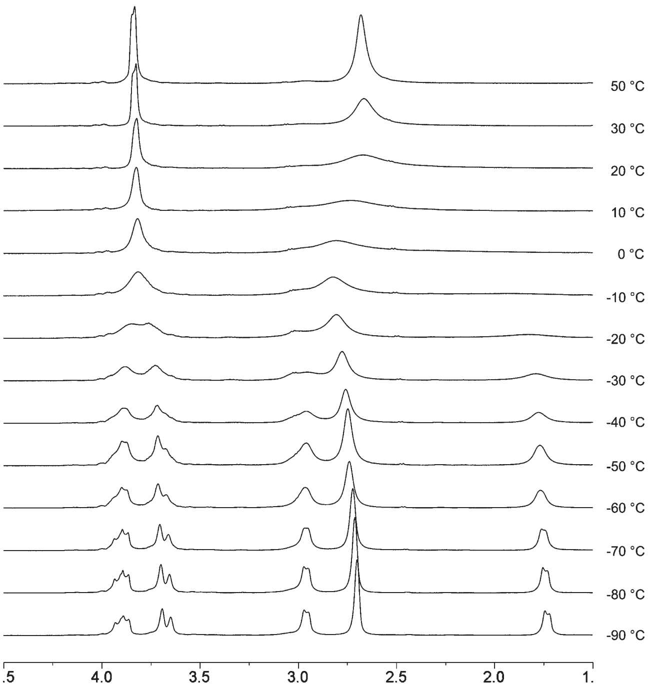

Figure 7. Variable-temperature ^1H NMR spectra (400 MHz, CD_2Cl_2) of $(^{CF_3}PCP)Ir(C_2H_4)_2$ (**4**).

The observation of a single ethylene resonance at 2.70 ppm for one of the ethylene ligands in $(^{CF_3}PCP)Ir(C_2H_4)_2$ at −90 °C implies that the barriers to ethylene rotation in **4** may be quite different.[17] To investigate this further, a DFT geometry optimization and subsequent energy calculation for **4** at the B97-1/cc-pVDZ level of theory was carried out (see the Experimental Section). While the reaction profiles for ethylene rotation and dissociation were not examined, the calculated structure (Figure 8) shows a substantial difference in axial and equatorial ethylene bond lengths. The significantly lengthened C−C bond (1.44 Å) and shorter Ir−C bond lengths (2.18, 2.17 Å) for the equatorial ethylene are consistent with the X-ray structure of the cod chelating analogue **11** (see Crystallographic Studies) and suggest increased back-bonding and a higher equatorial $Ir-C_2H_4$ rotational barrier. The C−C bond of the equatorial ethylene ligand is aligned with the P−Ir−P plane, analogous to the orientation of ethylene in $(^{CF_3}PCP)Ir(PhCN)(C_2H_4)$. The orientation of the axial ethylene ligand is canted 41° with respect to the PCP arene ring and is essentially along one of the Ir−P bonds; the orientation of the corresponding cod double bond in **11** in comparison is restricted by the chelate ring to ~12° out of the arene plane.

---

(16) Schnabel, R. C.; Roddick, D. M. *Organometallics* **1993**, *12*, 704–711.

[17] In the absence of an observed slow-exchange limit, this assumes a $\Delta\nu$ difference comparable to that found for the other ethylene ligand.

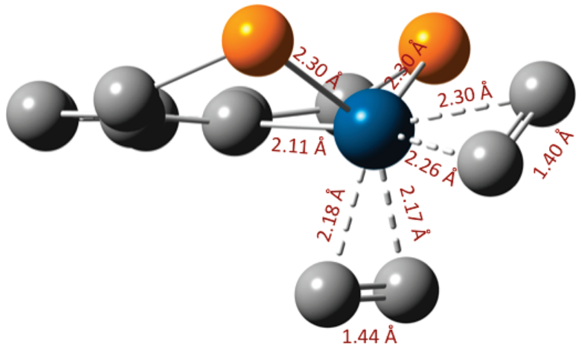

Figure 8. DFT geometry optimization for $(^{CF_3}PCP)Ir(C_2H_4)_2$ (**4**), showing asymmetrical axial and equatorial ethylene binding interactions.

Scheme 2

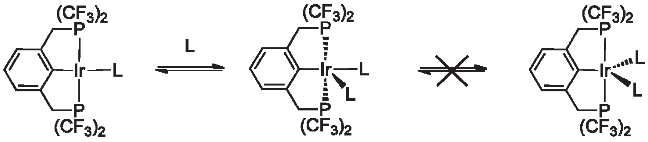

$(^{CF_3}PCP)Ir(PhCN)(C_2H_4)$ (**13**) exhibits slow exchange limit NMR spectra at 20 °C. At higher temperatures, coalescence of benzylic CH_2, inequivalent geminal C_2H_4, and CF_3 groups takes place. Kinetic fitting gives identical barriers for benzyl (16.1(2) kcal mol^{-1}, 50 °C) and CF_3 (16.1(2) kcal mol^{-1}, 90 °C) groups and a slightly lower barrier for ethylene site exchange (15.1(2) kcal mol^{-1}, 50 °C). The equilibration of diastereotopic groups in the asymmetrical complex $(^{CF_3}PCP)Ir(L)(L')$ is not consistent with intramolecular ligand site exchange involving L and L′ in equatorial positions and supports a dissociative mechanism (Scheme 2). Further support for a dissociative ligand site exchange mechanism for $(^{CF_3}PCP)Ir(L)_2$ systems is provided by the chelate complexes **10**−**12**, which exhibit NMR spectra reflecting a static five-coordinate environment with inequivalent chelate ends at ambient temperatures. No changes in NMR spectra for **12** were observed up to 100 °C.

A dissociative mechanism for $(^{CF_3}PCP)Ir(L)_2$ ligand site exchange relates the observed exchange barriers to $(^{CF_3}PCP)Ir(L)-L$ bond dissociation energies: 9.7 kcal mol^{-1} for $(^{CF_3}PCP)Ir(CO)-CO$ and 12.2 kcal mol^{-1} for $(^{CF_3}PCP)Ir(C_2H_4)-C_2H_4$.[18] For comparison, DFT calculations for $(^{pyr}PCP)Rh(CO)_2$ predict that the loss of equatorial CO is 2.2−3.4 kcal mol^{-1} uphill.[15] A higher dissociation energy of 16.1 kcal mol^{-1} is implicated for $(^{CF_3}PCP)Ir(NCPh)(C_2H_4)$, but in this unsymmetrical molecule further data are required to determine whether benzonitrile or ethylene is preferentially dissociated.

$(^{CF_3}PCP)Ir(L)$ Oxidative Addition Reactions. The 16-electron Ir(I) systems *trans*-$(R_3P)_2Ir(L)(X)$ commonly undergo oxidative addition reactions with both polar and nonpolar reactants. Accordingly, complex **1** reacts with an excess of MeI in benzene to afford $(^{CF_3}PCP)Ir(CO)(CH_3)I$ (**14**) (eq 5). The trans disposition of methyl and iodide ligands in **14** has been confirmed by X-ray diffraction (see the Supporting Information). The donor PCP complex $(^{iPr}PCP)Ir(CO)$ has been reported to readily react with methyl iodide to form a $(^{iPr}PCP)Ir(CO)(CH_3)I$ product with analogous stereochemistry.[19]

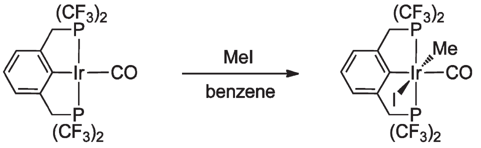

14 (5)

In contrast to the oxidative addition of ionizable substrates A−B to d^8 square-planar systems, which generally result in kinetic products with trans A and B groups, the oxidative addition reactions with dihydrogen proceed via η-H_2 intermediates and lead to kinetic and usually thermodynamically preferred *cis*-dihydride products. In contrast to this expectation, Milstein has reported that treatment of $(^{iPr}PCP)Ir(CO)$ with H_2 reversibly affords the expected *cis*-dihydride product *cis*-$(^{iPr}PCP)Ir(CO)(H)_2$, which then slowly rearranges upon heating at 90 °C under 35 psi of H_2 to *trans*-$(^{iPr}PCP)Ir(CO)(H)_2$ as the thermodynamically preferred isomer. The reaction of $(^{CF_3}PCP)Ir(CO)$ with H_2 has distinctly different kinetic behavior: exposure of orange benzene solutions of **1** to 1 atm of hydrogen at ambient temperatures resulted in a rapid bleaching and the direct formation of *trans*-$(^{CF_3}PCP)Ir(CO)(H)_2$ (**15**) (eq 6). Removal of hydrogen rapidly converted **15** back to **1**. ^1H NMR spectra of **15** exhibit a diagnostic hydride triplet at −9.10 ($^2J_{HP}$ = 19.2 Hz) and a single benzylic resonance which, together with the chemical equivalence of CF_3 groups in ^{19}F spectra, confirms the symmetrical trans stereochemistry.

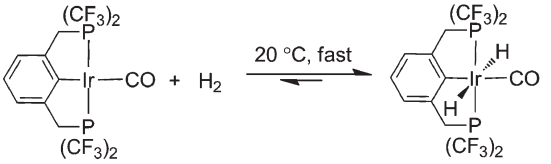

15 (6)

The reaction of the dfmp complex **5** with H_2 is quite different (eq 7). Under 1 atm of H_2, **5** rapidly and reversibly converts at 20 °C to the dihydride product $(^{CF_3}PCP)Ir(dfmp)(H)_2$ (**16**), which displays a single complex hydride multiplet at δ −11.45 as well as diasterotopic benzylic resonances and inequivalent CF_3 ^{19}F doublets. These features are inconsistent with either the cis or trans dihydride stereochemistry expected for a meridional $(^{CF_3}PCP)Ir$ pincer ancillary unit. At ambient temperatures the new species **17** slowly grows in with an associated hydride resonance at δ −10.18 (∼10% conversion, 24 h), which reaches a maximum conversion of 30% after 3 days. No further change in the **16**/**17** ratio was observed after 2 weeks at ambient temperature or after subsequent warming to 80 °C for 1 week. We assign **17** as the minor *trans*-dihydride isomer *mer*, *trans*-$(^{CF_3}PCP)Ir(dfmp)(H)_2$ (**17**). ^{31}P decoupling experiments and simulation of the hydride resonance for **16** define a AA′MXX′ spin system with cis hydride ligands (A, A′) coplanar with cis pincer $P(CF_3)_2$ groups (X, X′) and a mutually cis dfmp phosphorus (M). The facial pincer coordination geometry indicated for **16** by NMR data is quite

---

[18] An explanation for the small but significant discrepancy in activation values for the bis-ethylene system is not readily apparent; we adopt an averaged value here.

[19] Rybtchinski, B.; Ben-David, Y.; Milstein, D. *Organometallics* **1997**, *16*, 3786–3793.

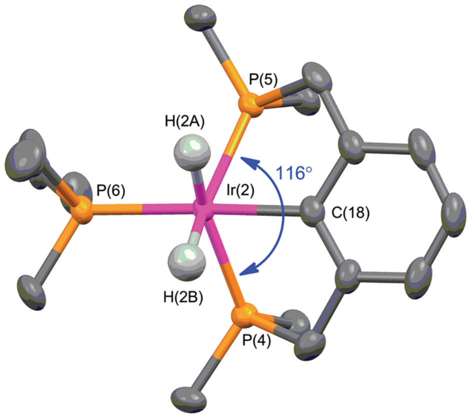

Figure 9. Molecular structure of *fac,cis*-(^{CF_3}PCP)Ir(dfmp)(H)$_2$ (**16**) with 50% probability thermal ellipsoids. Hydrogen atoms (except hydride ligands) and fluorine atoms are omitted for clarity. Selected bond distances (Å) and angles (deg) for **16**: Ir(2)−C(18) = 2.121(4), Ir(2)−P(6) = 2.2904(11), Ir(2)−P(4) = 2.2942(10), Ir(2)−P(5) = 2.3028(10), Ir(2)-H(2A) = 1.51(5), Ir(2)-H(2B) = 1.51(5); C(18)−Ir(2)−P(6) = 170.99(10), C(18)−Ir(2)−P(4) = 77.15(11), P(6)−Ir(2)−P(4) = 105.16(4), C(18)−Ir(2)−P(5) = 77.05(11), P(6)−Ir(2)−P(5) = 108.97(4), P(4)−Ir(2)−P(5) = 116.30(4), H(2A)−Ir(2)−H(2B) = 85(3).

unusual and has been confirmed by X-ray crystallography (Figure 9).

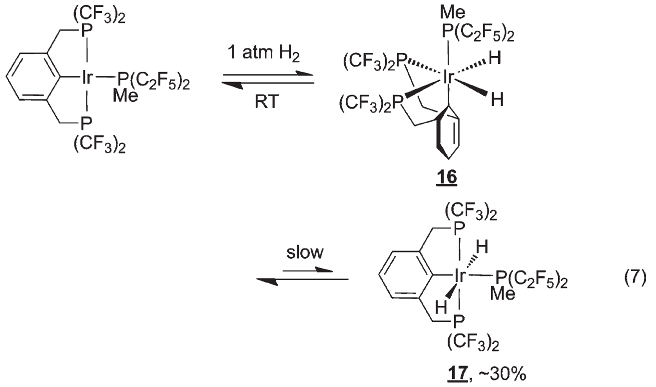

The existence of the stable *fac,cis*-dihydride **16** led us to examine the course of reaction of (^{CF_3}PCP)Ir(CO) (**1**) with H$_2$ by variable-temperature NMR (Figure 10). Upon mixing of **1** with 3 atm of H$_2$ in acetone-d_6 at −60 °C, a single product is observed with a AA′XX′ hydride resonance at δ −9.79 ($^2J_{PH}$ = −157, 33 Hz) which is assigned as *fac*, *cis*-(^{CF_3}PCP)Ir(CO)(H)$_2$ (**18**). When the temperature is raised, coalescence is observed near −40 °C and then a sharpening occurs to form a single broadened singlet ($\nu_{1/2}$ = 22 Hz, T_1 = 1.72 s) at −20 °C. At higher temperatures this resonance broadens and coalesces into the baseline by 20 °C. At temperatures above −20 °C, the resonance at δ 4.54 due to dissolved free H$_2$ also broadens, due to exchange with **18**. Modeling intermolecular proton exchange between **18** and **1** is not straightforward. However, this exchange process correlates with the intramolecular site exchange of diastereotopic PCP benzyl protons and CF$_3$ groups. At −60 °C, ^{19}F NMR spectra for **18** show distinct CF$_3$ doublets at −59.9 and −62.3 ppm which coalesce at −20 °C, corresponding to $\Delta G^{\ddagger}$ = 10.9(2) kcal mol^{-1} . Modeling the coalescence behavior of the benzylic protons gives an essentially identical value of $\Delta G^{\ddagger}$ = 11.0(2) kcal mol^{-1}. At −40 °C, new triplet hydride resonances at δ −11.28 ($^2J_{PH}$ = 18 Hz) and δ −11.71 ($^2J_{PH}$ = 15 Hz) begin to appear, which are assigned to *mer*, *cis*-(^{CF_3}PCP)Ir(CO)(H)$_2$ (**19**) The *cis*-dihydride **19** reaches a maximum integrated intensity at 0 °C of 1.5/1 with respect to **18** and then decays as the thermodynamically preferred trans hydride product **15** forms with warming above 0 °C. After 15 min at 20 °C a 5.9/1 ratio of **15** to **19** is established.

These observations are consistent with a reaction mechanism involving the reversible addition of H$_2$ to (^{CF_3}PCP)-Ir(CO) and a kinetic preference for H$_2$ addition across the P−Ir−P axis to form *fac,cis*-(^{CF_3}PCP)Ir(CO)(H)$_2$ (**18**) (Scheme 3). At higher temperatures the hydride resonance for **18** is further broadened due to exchange with free H$_2$. Addition of H$_2$ across the C−Ir−CO axis has a larger kinetic barrier and leads to the formation of *mer,cis*-(^{CF_3}PCP)Ir-(CO)(H)$_2$ at higher temperatures. Stereochemical preferences for H$_2$ addition across *trans*-(R$_3$P)$_2$Ir(CO)X systems are well-known.[20] The mechanism of formation of the final *trans*-dihydride product **15** is not certain. Brookhart has recently reported base-assisted isomerization of *cis*-(PNP)Ir-(Me)(H)$_2$ to *trans*-(PNP)Ir(Me)(H)$_2$ involving deprotonation/reprotonation by adventitious water.[21] Addition of 2 equiv of H$_2$O resulted in no significant change in the rate of isomerization from **19** to **15**. Calculations by Hall suggest that an intramolecular "trigonal twist" mechanism connecting *cis*- and *trans*-dihydride isomers is energetically accessible.[22] A trigonal twist mechanism, which requires a facial PCP distortion accompanying a turnstyle-type twisting of the P$_1$, H$_1$, and H$_2$ groups (see labeling in Scheme 3), should be favored for electron-withdrawing pincer ligands and is consistent with the low isomerization barrier found for (^{CF_3}PCP)Ir(CO)(H)$_2$.

Crystallographic Studies. Crystallographic data obtained for a range of four-, five-, and six-coordinate (^{CF_3}PCP)Ir complexes allows us to compare pincer structural features with donor PCP systems (Table 1). Following established electronic effects for phosphines containing π-accepting perfluoroalkyl substituents,[8,16,23] Ir−P(^{CF_3}PCP) bonds for (^{CF_3}PCP)Ir(L) complexes (complexes **1**, **2**, **5**, and **7**) average 2.212 Å, which is significantly shorter than the Ir−P bond length average of 2.296 Å for ^{R}PCP as well as ^{R}POCOP systems.[2i,10,24] The average Ir−P(^{CF_3}PCP) bond length for five-coordinate Ir(I) systems (complexes **3**, **6**, and **11**−**13**) is slightly longer (2.252 Å). The average Ir−C(^{CF_3}PCP) bond distance is 2.084 Å, which is on the high end of the 2.001−2.102 Å range found for donor pincer structures.

---

(20) Deutsch, P. P.; Eisenberg, R. *Chem. Rev.* **1988**, *88*, 1147–1161.

(21) Findlater, M.; Bernskoetter, W. H.; Brookhart, M. *J. Am. Chem. Soc.* **2010**, *132*, 4534–4535.

(22) Li, S.; Hall, M. B. *Organometallics* **1999**, *18*, 5682–5687.

(23) (a) Ernst, M. F.; Roddick, D. M. *Organometallics* **1990**, *9*, 1586–1594. (b) Schnabel, R. C.; Roddick, D. M. *Inorg. Chem.* **1993**, *32*, 1513–1518. (c) Butikofer, J. L.; Hoerter, J. M.; Peters, R. G.; Roddick, D. M. *Organometallics* **2004**, *23*, 400–408. (d) Adams, J. J.; Lau, A.; Arulsamy, N.; Roddick, D. M. *Inorg. Chem.* **2007**, *46*, 11328–11334.

(24) (a) Lee, D. W.; Kaska, W. C.; Jensen, C. M. *Organometallics* **1998**, *17*, 1–3. (b) Morales-Morales, D.; Redon, R.; Wang, Z.; Lee, D. W.; Yung, C.; Magnuson, K.; Jensen, C. M. *Can. J. Chem.* **2001**, *79*, 823–829. (c) Kanzelberger, M.; Zhang, X.; Emge, T. J.; Goldman, A. S.; Zhao, J.; Incarvito, C.; Hartwig, J. F. *J. Am. Chem. Soc.* **2003**, *125*, 13644–13645. (d) Cartwright Sykes, A.; White, P.; Brookhart, M. *Organometallics* **2006**, *25*, 1664–1675. (e) Ghosh, R.; Kanzelberger, M.; Emge, T. J.; Hall, G. S.; Goldman, A. S. *Organometallics* **2006**, *25*, 5668–5671. (f) Ghosh, R.; Zhang, X.; Achord, P.; Emge, T. J.; Krogh-Jespersen, K.; Goldman, A. S. *J. Am. Chem. Soc.* **2007**, *129*, 853–866.

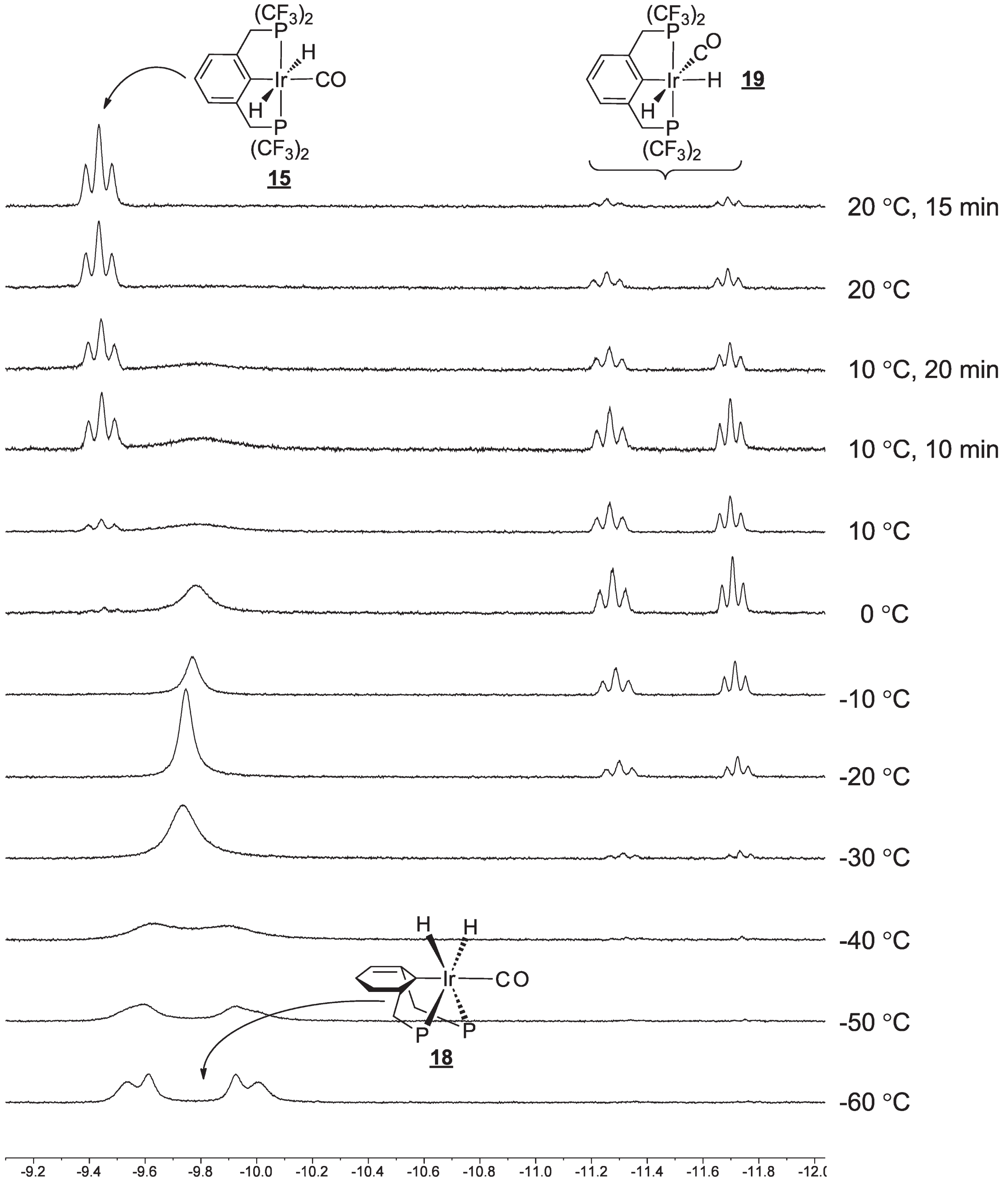

Figure 10. Variable-temperature ^{1}H NMR spectra (400 MHz, acetone-d_6) of (^{CF_3}PCP)Ir(CO) (**1**) under 3 atm of H_2, with hydride resonance assignments.

Structurally characterized four-coordinate (pincer)M(η^2-alkene) systems have been reported.[8,25] With the exception of the bulky phosphite compounds (^{biphenol}POCOP)Rh(η^2-C_2H_4), all alkene complexes show a significant rotation of the M−alkene moiety out of the (pincer)M plane. The norbornene complex **7** exhibits an unusual disposition of the alkene ligand and the pincer ancillary ligand. Rather than a simple rotation about the Ir−alkene centroid, the plane defined by the iridium and the norbornene vinylic carbons is not rotated but is instead *canted* 17.3° below the pincer aryl plane. This distortion tilts the norbornene CH_2 away from the pincer CF_3 groups. In addition, the P−Ir−P angle, 142.3°, is not just bent away from the fourth ligand, which is typical for pincer four-coordinate complexes, but is much smaller than the 155−159° values for other (^{CF_3}PCP)Ir(L) systems, due to a distortion *above* the (aryl)Ir plane. This flexibility of the (^{CF_3}PCP)Ir moiety also allows the P(CF_3) groups syn to the norbornene bridging methylene to ease their steric interactions and is consistent with the high level of ligand stereochemical flexibility reflected in the five-coordinate (^{CF_3}PCP)Ir(L)$_2$ structures and in **16** (see below). The

---

(25) (a) Zhao, J.; Goldman, A. S.; Hartwig, J. F. *Science* **2005**, *307*, 1080–1082. (b) Ben-Ari, E.; Cohen, R.; Gandelman, M.; Shimon, L. J. W.; Martin, J. M. L.; Milstein, D. *Organometallics* **2006**, *25*, 3190–3210. (c) Rubio, M.; Suarez, A.; del Rio, D.; Galindo, A.; Alvarez, E.; Pizzano, A. *Dalton Trans.* **2007**, 407–409. (d) Yano, T.; Moroe, Y.; Yamashita, M.; Nozaki, K. *Chem. Lett.* **2008**, *37*, 1300–1301. (e) Friedrich, A.; Ghosh, R.; Kolb, R.; Herdtweck, E.; Schneider, S. *Organometallics* **2009**, *28*, 708–718. (f) Rubio, M.; Suarez, A.; del Rio, D.; Galindo, A.; Alvarez, E.; Pizzano, A. *Organometallics* **2009**, *28*, 547–560.

Scheme 3

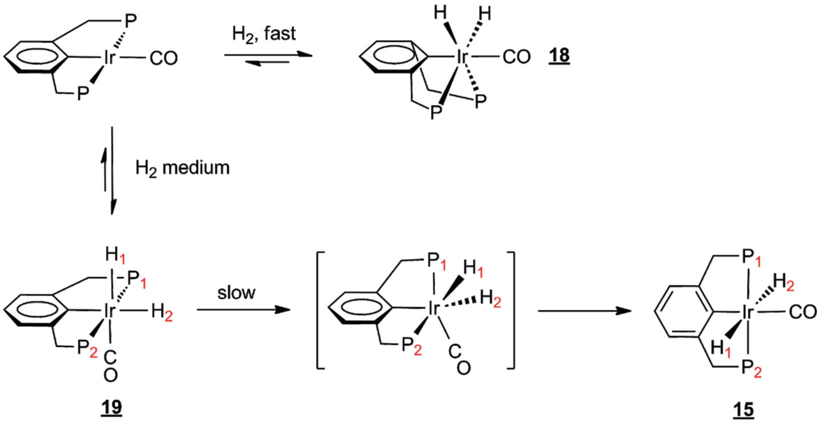

Table 1. Selected Bond Distances (Å) and Angles (deg) for (^{CF_3}PCP)Ir(L$_{ax}$) and (^{CF_3}PCP)Ir(L$_{ax}$)(L$_{eq}$) Complexes

complex	Ir−P(PCP)$_{av}$	Ir−C	Ir−L$_{ax}$	Ir−L$_{eq}$	P−Ir−P	L$_{ax}$−Ir−C	L$_{eq}$−Ir−C	L$_{eq}$−Ir−L$_{ax}$
(^{CF_3}PCP)Ir(CO) (**1**)	2.224	2.088(1)	1.895(2)		159.3	179.1		
(^{CF_3}PCP)Ir(DBU) (**2**)	2.189	2.047(4)	2.135(3)		158.3	178.1		
(^{CF_3}PCP)Ir(dfmp) (**5**)	2.237	2.118(3)	2.255(1)		155.5	177.3		
(^{CF_3}PCP)Ir(nbe) (**7**)	2.196	2.089(2)	2.157[a]		142.3	166.1[a]		
(^{CF_3}PCP)Ir(CO)$_2$ (**3**)	2.247	2.131(3)	1.939(4)	1.941(4)	130.3	171.6	91.6	96.7
(^{CF_3}PCP)Ir(dfmp)$_2$ (**6**)	2.264	2.138(2)	2.312(1)	2.309(1)	124.2	173.6	84.4	101.9
(^{CF_3}PCP)Ir(cod) (**11**)	2.261	2.097(4)	2.192[a]	2.046[a]	119.0	173.0[a]	89.4[a]	84.2[a]
(^{CF_3}PCP)Ir(dfepe) (**12**)	2.269	2.146(2)	2.300(1)	2.288(1)	126.2	177.1	96.4	83.2
(^{CF_3}PCP)Ir(NCPh)(C$_2$H$_4$) (**13**)	2.221	2.057(4)	2.088(3)	2.059[a]	123.8	177.9	90.2[a]	90.7[a]

[a] Calculated using the centroids of the alkene ligand.

observed C=C bond length for **7**, 1.394(4) Å, is similar to that for the more electron-rich complex [((tBu)$_2$PCH$_2$CH$_2$C(H)CH$_2$CH$_2$P(^{t}Bu)$_2$]Ir(η^2-propene) (1.402(6) Å) and longer than that found for (^{CF_3}PCP)Pt(η^2-C$_2$H$_4$)$^+$ (1.305(7) Å).[8,25a]

Carbonyl complexes **1** and **3** and the dfmp complexes **5** and **6** provide an opportunity to compare closely related four- and five-coordinated d^8 geometries (Figures 2 and 3). Complexes **3** and **6**, in particular, follow Milstein's earlier report of the first five-coordinate d^8 pincer complexes, (^{pyr}PCP)Rh(PR$_3$)(CO).[15] Complexes **1** and **5** are essentially square planar, with a maximum deviation from the mean-square plane defined by iridium and the four attached atoms of 0.027 Å for **1** and 0.034 Å for **5**. The pincer P−Ir−P angles, 159.3° (**1**) and 155.5° (**5**), are canted away from the CO and dfmp ligands and are within the mean-square plane. Smaller P−M−P pincer angles correlate with increased steric interactions; consistent with this, a greater pincer C2 interplanar angle twist of 17.3° between the pincer arene ring and the coordination plane is found for **5** versus that for **1** (13.5°).

The five-coordinate complexes **3** and **6** adopt a distorted-trigonal-bipyramidal coordination geometry with axial CO (or dfmp) ligands and pincer C(aryl) groups (**3**, C(1)−Ir−C(13) = 171.6°; **6**, C(1)−Ir−P(4) = 173.6°, tilted away from the remaining CO (or dfmp) ligand). The equatorial CO in **3** has angles of C(1)−Ir−C(14) = 91.6° and C(1)−Ir−C(13) = 96.7°, and the P−Ir−P angle is 130.3°. For **6**, steric interactions bend the equatorial dfmp phosphorus P(3) away from the axial dfmp ligand; the corresponding angles are C(1)−Ir−P(3) = 84.4° and P(3)−Ir−P(4) = 101.9°, and the P−Ir−P angle is reduced to 124.2°. For comparison, the P−Rh−P pincer angle for (^{pyr}PCP)Rh(PEt$_3$)(CO) is 128.3°. Due to terdentate bonding constraints, the pincer phosphorus atoms in **3** and **6** are bent out of an idealized equatorial plane normal to the C(1)−Ir−L(axial) axis toward the arene group. In complex **6** the equatorial dfmp Ir−P(3) bond length (2.3089(4) Å) is slightly shorter than the axial dfmp Ir−P(4) bond length (2.3120(4) Å), and both are significantly longer than the pincer Ir−P bond lengths (2.2602(4), 2.2668(4) Å). The remaining five-coordinate structures display similar angular distortions, though complexes **11** and **12** are further constrained by the chelating cod and dfepe ligands.

The chelating cod complex **11** provides a revealing model for the bis-ethylene complex (^{CF_3}PCP)Ir(C$_2$H$_4$)$_2$ (**4**). Alkene coordination in **11** is quite asymmetrical: the double bond cis to the Ir−C(aryl) bond (equatorial) is significantly lengthened (C(13)−C(14) = 1.435(6) Å) with shorter Ir−C bonds (Ir(1)−C(13) = 2.162(4) Å; Ir(1)−C(14) = 2.175(4) Å) compared to the double bond trans to the aryl Ir−C bond (axial) (C(17)−C(18) = 1.375(6) Å; Ir(1)−C(17) = 2.295(4) Å; Ir(1)−C(18) = 2.299(4) Å). This reflects considerably greater metal back-bonding from the (^{CF_3}PCP)Ir^I moiety to the equatorial ligand. This asymmetry in back-bonding ability is not observed for dicarbonyl **3** and is only very slightly reflected in dfmp bond lengths for (^{CF_3}PCP)Ir(dfmp)$_2$ (**6**) (Ir−P(dfmp)$_{ax}$ − Ir−P(dfmp)$_{eq}$ = 0.003 Å) and (^{CF_3}PCP)Ir(dfepe) (**12**) (Ir−P(dfepe)$_{ax}$ − Ir−P(dfepe)$_{eq}$ = 0.013 Å). We tentatively ascribe the greater bonding asymmetry in bis-alkene complexes to a mismatch of optimal back-bonding and axial alkene orientation. Note added in proof: The X-ray structure of the bis ethylene complex **4** has now been determined, which similarly shows an elongated equatorial C−C ethylene bond (1.40 Å) and a shorter axial C−C bond (1.33 Å).

The *fac*-(R$_3$P)$_3$Ir(H$_2$)(X) coordination environment of **16** (Figure 7) is relatively rare.[26] The Ir−P bond lengths to P(5) and P(6), which are trans to hydride ligands, are 2.294(1) and 2.303(1) Å, somewhat longer than 2.189−2.269 Å range for meridionally coordinated $^{\mathrm{CF_3}}$PCP systems with trans phosphorus groups. These bond lengths reflect the greater hydride ligand trans influence and are comparable to the Ir−P values reported for *fac*-$(MePh_2P)_3IrH_3$ (2.314(2) Å) and *fac*-$(Me_3P)_3Ir(H)_2(SiHPh_2)$ (2.308(3), 2.310(30 Å).[26] The P-(4)−Ir(2)−P(5) PCP angle, 116.3°, is somewhat smaller than the range of 119−130° found for distorted bipyramidal ($^{\mathrm{CF_3}}$PCP)Ir$(L)_2$ structures (Table 1) but much greater than the ~100° angle found in unconstrained *fac*-$(R_3P)_3Ir(H_2)(X)$ structures. The osmium piano-stool complex Cp′Os($^{\mathrm{Ph}}$PCP)-Cl with a PCP P−Os−P angle of 113.2° has been reported.[27]

Summary

Interest in terdentate "pincer" ligands with a central aryl anchoring group is often attributed to their enhanced ancillary ligand stability as well as their preference for a coplanar coordination environment. This coplanarity is seen in: (1) three-coordinate "T-shaped" (pincer)M intermediates,[2c,28] (2) four-coordinate square-planar (pincer)M(L) systems, and (3) six-coordinate meridional octahedral geometries, (pincer)M(L)(X)(Y). In addition to the ubiquitous square-planar d^8 Ir(I) systems, $(L)_3Ir(X)$, examples of five-coordinate complexes such as $(PPh_3)_3Ir(CO)(H)$[29] and $(dppe)_2Ir(CO)^+$ are known;[30] until now, none containing the $(PCP)Ir^I$ moiety have been prepared. Following Milstein's report of five-coordinate ($^{\mathrm{pyr}}$PCP)Rh(PR_3)(CO) systems,[15] the present work demonstrates that ($^{\mathrm{CF_3}}$PCP)Ir$(L)_2$ systems possessing the strongly π-accepting $P(CF_3)_2$ groups spanning equatorial coordination sites in a distorted-trigonal-bipyramidal geometry are quite stable. In a simplistic sense, this pincer distortion allows the acceptor phosphine centers to reduce trans ligand competition for dπ back-bonding density.

The unusual hydrogen addition products *fac*,*cis*-($^{\mathrm{CF_3}}$PCP)Ir(dfmp)$(H)_2$ (**16**) and *fac*,*cis*-($^{\mathrm{CF_3}}$PCP)Ir(CO)-$(H)_2$ (**18**) are also consistent with the enhanced ability of acceptor PCP ligands to adopt a noncoplanar coordination geometry. The apparent thermodynamic preference for *cis*-dihydride coordination in **16** is in contrast with the preference for the trans carbonyl dihydride product **15**. Scheme 3, besides rationalizing VT NMR results for the reaction of ($^{\mathrm{CF_3}}$PCP)Ir(CO) and H_2, also suggests an explanation for the surprising steric sensitivity of H_2 addition to ($^{\mathrm{R}}$PCP)Ir(CO) (R = ^{i}Pr, ^{t}Bu), which is indicated by the failure of ($^{t\mathrm{Bu}}$PCP)Ir(CO) to react with H_2.[2d] The initial formation of a trigonal-bipyramidal H_2 adduct requires pincer bending, which would force an unfavorable interaction of the syn bulky ^{t}Bu groups. It is apparent that both steric and electronic influences of pincer phosphine substituents should be considered in ligand addition reactions to (PCP)Ir(L) systems.

From the standpoint of pincer coordination chemistry, the ability of acceptor pincer ligands to support a broader range of ancillary coordination geometries opens up new avenues for future research. In a forthcoming paper we shall report the application of ($^{\mathrm{CF_3}}$PCP)Ir$(L)_x$ systems to alkane dehydrogenation and aldehyde decarbonylation catalysis.

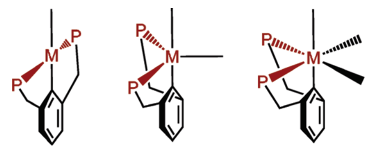

Experimental Section

General Procedures. All manipulations were conducted under N_2 or vacuum using high-vacuum-line and glovebox techniques, unless otherwise noted. All ambient-pressure chemistry was carried out under a pressure of approximately 590 Torr (elevation ~2195 m). All solvents were dried using standard procedures and stored under vacuum. Aprotic deuterated solvents used in NMR experiments were dried over activated 3 Å molecular sieves. Elemental analyses were performed by Desert Analytics or Columbia Analytical Services. NMR spectra were obtained with a Bruker DRX-400 instrument using 5 mm NMR tubes fitted with Teflon valves (Chemglass CG-512 or New Era CAV-VBP). ^{31}P spectra were referenced to an 85% H_3PO_4 external standard. ^{19}F spectra were referenced to $CF_3CO_2CH_2CH_3$ (δ −75.32) and $CF_3C_6H_5$ external standards. The gases CO (Airgas), C_2H_4 (Airgas), and H_2 (UHP, Praxair) were purchased and used without further purification; all other reagents were purchased from Aldrich and were used without further purification. The complexes ($^{\mathrm{CF_3}}$PCP)Ir(CO)(H)Cl, ($^{\mathrm{CF_3}}$PCP)Ir(C_2H_4)(H)Cl, ($^{\mathrm{CF_3}}$PCP)Ir(MeCN)(H)Cl, ($^{\mathrm{CF_3}}$PCP)-Ir(PhCN)(H)Cl, and ($^{\mathrm{CF_3}}$PCP)Ir$(MeP(C_2F_5)_2)$(H)Cl were prepared by following procedures described in the previous paper.[7]

(CF_3PCP)Ir(CO) (1). (CF_3PCP)Ir(CO)(H)Cl (0.500 g, 0.716 mmol) and Et_3N (144 μL, 0.104 g, 1.432 mmol) were dissolved in 15 mL of C_6H_6. The initially colorless solution rapidly turned orange, and a white precipitate was observed. After the reaction mixture was stirred at ambient temperature for 12 h, the volatiles were removed under vacuum, 10 mL of hexanes was added, and the solution was filtered to remove $Et_3NH^+Cl^-$. Cooling the filtrate to −78 °C afforded an orange precipitate, which was collected via cold filtration and dried under vacuum (0.330 g, 70% yield). Crystals suitable for X-ray diffraction were grown by slow evaporation from a 1/2 pentafluoropyridine/perfluoro-2-butyltetrahydrofuran solution. Anal. Calcd for $C_{13}H_7P_2F_{12}OIr$: C, 23.57; H, 1.07. Found: C, 23.94; H, 0.71. ^{1}H NMR (C_6D_6, 400.13 MHz, 20 °C): δ 6.90 (t, $^3J_{HH}$ = 8 Hz, 1H; *p*-$C_6H_3(CH_2P(CF_3)_2)_2$), 6.79 (d, $^3J_{HH}$ = 8 Hz, 2H; *m*-$C_6H_3(CH_2P(CF_3)_2)_2$), 3.29 (m, 4H; $C_6H_3(CH_2P(CF_3)_2)_2$). $^{31}P\{^1H\}$ NMR (C_6D_6, 161.97 MHz, 20 °C): δ 69.6 (m). ^{19}F NMR (C_6D_6, 376.50 MHz, 20 °C): δ −57.5 (m, 12F; PCF_3). IR (CH_2Cl_2): ν(CO) 2018 cm^{-1}.

($^{\mathrm{CF_3}}$PCP)Ir(DBU) (2). ($^{\mathrm{CF_3}}$PCP)Ir(MeCN)(H)Cl (0.450 g, 0.633 mmol) and DBU (1,8-diazabicyclo[5.4.0]undec-7-ene, 142 μL, 0.145 g, 0.949 mmol) were dissolved in 10 mL of C_6H_6. The reaction mixture was stirred at ambient temperature for 12 h, during which time the solution changed from colorless to red. Volatiles were removed, and ca. 20 mL of petroleum ether was added. The solution was filtered away from unreacted starting material and protonated DBU. The red filtrate was cooled to −78 °C, and a red precipitate formed, which was collected by filtration (0.221 g, 59% yield). Crystals suitable for X-ray diffraction were grown by slow evaporation from a 1/2 pentafluoropyridine/perfluoro-2-butyltetrahydrofuran solution. Anal. Calcd for $C_{21}H_{23}P_2F_{12}N_2Ir$: C, 32.06; H, 2.95, N, 3.56. Found: C, 32.06, H, 2.44; N, 3.56. ^{1}H NMR (C_6D_6, 400.13 MHz,

---

[26] (a) Zarate, E. A.; Kennedy, V. O.; McCune, J. A.; Simons, R. S.; Tessier, C. A. *Organometallics* **1995**, *14*, 1802–1809. (b) Bau, R.; Schwerdtfeger, C. J.; Garlaschelli, L.; Koetzle, T. F. *J. Chem. Soc., Dalton Trans.* **1993**, 3359–3362.

[27] Wen, T. B.; Zhou, Z. Y.; Jia, G. *Angew. Chem., Int. Ed.* **2006**, *45*, 5842–5846.

[28] (a) Krogh-Jespersen, K.; Czerw, M.; Goldman, A. S. *J. Mol. Catal. A: Chem.* **2002**, *189*, 95–110. (b) Goettker-Schnetmann, I.; Brookhart, M. *J. Am. Chem. Soc.* **2004**, *126*, 9330–9338. (c) Krogh-Jespersen, K.; Czerw, M.; Goldman, A. S. *ACS Symp. Ser.* **2004**, *885*, 216–233.

[29] Bath, S. S.; Vaska, L. *J. Am. Chem. Soc.* **1963**, *85*, 3500–3501.

[30] (a) Sacco, A.; Rossi, M.; Nobile, C. F. *Chem. Commun.* (*London*) **1966**, 589–590. (b) Vaska, L.; Catone, D. L. *J. Am. Chem. Soc.* **1966**, *88*, 5324–5325.

20 °C): δ 6.99 (t, $^3J_{HH}$ = 8 Hz, 1H; p-$C_6H_3(CH_2P(CF_3)_2)_2$), 6.88 (d, $^3J_{HH}$ = 8 Hz, 2H; m-$C_6H_3(CH_2P(CF_3)_2)_2$), 3.46 (dt, $^2J_{HH}$ = 18 Hz, $^2J_{PH}$ = 5 Hz, 2H; $C_6H_3(CH_2P(CF_3)_2)_2$), 3.30 (m, 4H; DBU CH_2 overlapping $C_6H_3(CH_2P(CF_3)_2)_2$), 2.84 (m, 2H; DBU), 2.42 (m, 2H; DBU), 2.34 (t, $^3J_{HH}$ = 6 Hz, 2H; DBU), 1.44 (br. p, 2H; DBU), 1.31 (p, $^3J_{HH}$ = 6 Hz, 2H; DBU), 1.13 (br. m, 2H; DBU), 0.88 (m, 2H; DBU). $^{31}P\{^1H\}$ NMR (C_6D_6, 161.97 MHz, 20 °C): δ 58.0 (m). ^{19}F NMR (C_6D_6, 376.50 MHz, 20 °C): δ −60.2 (m, 6F; PCF_3), −60.6 (m, 6F; PCF_3).

$(^{CF_3}PCP)Ir(CO)_2$ (3). $(^{CF_3}PCP)Ir(CO)(H)Cl$ (0.250 g, 0.359 mmol) and Et_3N (150 μL, 0.108 g, 1.076 mmol) were dissolved in 15 mL of C_6H_6. One atmosphere of CO was introduced into the reaction mixture, and it was stirred for 20 h at ambient temperature. The reaction mixture remained colorless, giving a white $HNEt_3^+Cl^-$ precipitate. The salt was removed via filtration, and the volatiles were removed, giving an orange oil. Hexane (20 mL) was added to the oil, and 1 atm of CO was introduced, giving a colorless solution with a small amount of solid. The solid was filtered away and the filtrate cooled to −78 °C to give **3** as an elementally pure white solid which was collected via cold filtration (0.210 g, 85% yield). Crystals suitable for single-crystal X-ray diffraction were grown by slow evaporation from a 1/4 benzene/hexanes solution at −30 °C. Anal. Calcd for $C_{14}H_7P_2F_{12}O_2Ir$: C, 24.35; H, 1.02. Found: C, 24.39; H, 0.99. *20 °C NMR data*: ^1H NMR (C_6D_6, 400.13 MHz) δ 6.72 (d, $^3J_{HH}$ = 8 Hz, 2H; m-$C_6H_3(CH_2P(CF_3)_2)_2$), 6.59 (t, $^3J_{HH}$ = 8 Hz, 1H; p-$C_6H_3(CH_2P(CF_3)_2)_2$), 3.24 (m, 4H; $C_6H_3(CH_2P(CF_3)_2)_2$); $^{31}P\{^1H\}$ NMR (C_6D_6, 161.97 MHz) δ 47.0 (m); ^{19}F NMR (C_6D_6, 376.50 MHz) δ −63.0 (d, $^2J_{FP}$ = 79 Hz, 12F; PCF_3). *−95 °C NMR data*: ^1H NMR (CD_2Cl_2, 400.13 MHz) δ 7.12 (d, $^3J_{HH}$ = 8 Hz, 2H; m-$C_6H_3(CH_2P(CF_3)_2)_2$), 6.97 (t, $^3J_{HH}$ = 8 Hz, 1H; p-$C_6H_3(CH_2P(CF_3)_2)_2$), 4.17 (dd, $^2J_{HH}$ = 17 Hz, $^2J_{HP}$ = 12 Hz, 2H; $C_6H_3(CH_2P(CF_3)_2)_2$), 3.83 (d, $^2J_{HH}$ = 17 Hz, 2H; $C_6H_3(CH_2P(CF_3)_2)_2$); $^{31}P\{^1H\}$ NMR (CD_2Cl_2, 161.97 MHz, 20 °C) δ 45.6 (m); ^{19}F NMR (CD_2Cl_2, 376.50 MHz, 20 °C) δ −65.4 (d, $^2J_{FP}$ = 76 Hz, 12F; PCF_3), −61.4 (d, $^2J_{FP}$ = 77 Hz, 12F; PCF_3). IR (CH_2Cl_2, cm^{-1}): ν(CO) 2068, 2020 cm^{-1}.

$(^{CF_3}PCP)Ir(C_2H_4)_2$ (4). An NMR tube was charged with ca. 15 mg of $(^{CF_3}PCP)Ir(C_2H_4)(H)Cl$ (0.021 mmol) and 0.5 mL of C_6D_6. Et_3N (2.8 μL, 0.002 g, 0.210 mmol) was syringed into the tube, and C_2H_4 (1 atm) was introduced into the NMR tube. After 24 h $Et_3NH^+Cl^-$ precipitated. A single major species, tentatively identified as **4**, was observed. For low-temperature spectra, the benzene solution was decanted away from the ammonium salt, the volatiles were removed under vacuum, and CD_2Cl_2 was added. *20 °C NMR data*: ^1H NMR (CD_2Cl_2, 400.13 MHz) δ 7.08 (d, $^3J_{HH}$ = 8 Hz, 2H; m-$C_6H_3(CH_2P(CF_3)_2)_2$), 6.93 (t, $^3J_{HH}$ = 8 Hz, 1H; p-$C_6H_3(CH_2P(CF_3)_2)_2$), 3.82 (br s, 4H; $C_6H_3(CH_2P(CF_3)_2)_2$), 2.68 (s, br ($\nu_{1/2}$ = 115 Hz), 8H; $Ir(C_2H_4)$); $^{31}P\{^1H\}$ NMR (C_6D_6, 161.97 MHz): δ 47.0 (m); $^{13}C\{^1H\}$ NMR (CD_2Cl_2, 100.61 MHz): δ 140.6 (m; C_{Ar}-Ir), 125.2 (s; *para*-$C_6H_3(CH_2P(CF_3)_2)_2$), 122.7 (m; *meta*-$C_6H_3(CH_2P(CF_3)_2)_2$), 46.0 (s; $Ir(C_2H_4)_2$), 39.1 (m; $CH_2P(CF_3)_2$); ^{19}F NMR (C_6D_6, 376.50 MHz) δ −57.9 (br m, 6F; PCF_3), −63.4 (br m, 6F; PCF_3). *−90 °C NMR data*: ^1H NMR (CD_2Cl_2, 400.13 MHz) δ 7.03 (d, $^3J_{HH}$ = 6 Hz, 2H; m-$C_6H_3(CH_2P(CF_3)_2)_2$), 6.89 (d, $^3J_{HH}$ = 6 Hz, 1H; p-$C_6H_3(CH_2P(CF_3)_2)_2$), 3.90 (dd, $^2J_{HH}$ = 18 Hz, $^2J_{HP}$ = 11 Hz, 2H; $C_6H_3(CH_2P(CF_3)_2)_2$), 3.67 (d, $^2J_{HH}$ = 18 Hz, 2H; $C_6H_3(CH_2P(CF_3)_2)_2$), 2.95 (br d, $^2J_{HH}$ = 9 Hz, 2H; $Ir(C_2H_4)$), 2.70 (br s, 4H; $Ir(C_2H_4)$), 1.73 ((br d, $^2J_{HH}$ = 9 Hz, 2H; $Ir(C_2H_4)$); $^{31}P\{^1H\}$ NMR (CD_2Cl_2, 161.97 MHz) δ 45.6 (m); $^{13}C\{^1H\}$ NMR (CD_2Cl_2, 100.61 MHz) δ 150.6 (s; C_{Ar}-$CH_2P(CF_3)_2$), 139.9 (m; C_{Ar}-Ir), 124.7 (d, $^1J_{CH}$ = 162 Hz; p-$C_6H_3(CH_2P(CF_3)_2)$, 122.7 (dd, $^1J_{CH}$ = 157 Hz, J_{CP} = 16 Hz; m-$C_6H_3(CH_2P(CF_3)_2)$, 45.1 (t, $^1J_{CH}$ = 163 Hz; $Ir(C_2H_4)_2$), 38.5 (tm, $^1J_{CH}$ = 141 Hz; $CH_2P(CF_3)_2$), 35.6 ((td, $^1J_{CH}$ = 16 Hz, $^2J_{CP}$ = 10 Hz; $Ir(C_2H_4)_2$); ^{19}F NMR (CD_2Cl_2, 376.50 MHz) δ −58.7 (d, $^2J_{FP}$ = 64 Hz, 6F; PCF_3), −65.4 (d, $^2J_{FP}$ = 64 Hz, 6F; PCF_3).

$(^{CF_3}PCP)Ir(dfmp)$ (5). $(^{CF_3}PCP)Ir(C_2H_4)(H)Cl$ (0.300 g, 0.430 mmol), Et_3N (0.25 mL, 0.185 g, 1.797 mmol), and $MeP(C_2F_5)_2$ (dfmp, 0.489 g, 1.720 mmol) were dissolved in benzene, and the reaction mixture was stirred at ambient temperature for 20 h. White $Et_3NH^+Cl^-$ precipitated and was filtered away, and the volatiles were removed, giving an orange oil. The oil was dissolved in 15 mL of hexane and filtered to remove a small amount of solid. The solution was reduced to a volume of ca. 5 mL and cooled to −78 °C, precipitating an orange solid (0.312 g, 79% yield). Crystals suitable for X-ray diffraction were grown by evaporating a hexane solution. Anal. Calcd for $C_{17}H_{10}P_3F_{22}Ir$: C, 22.26; H, 1.10. Found: C, 22.70; H, 1.19. ^1H NMR (C_6D_6, 400.13 MHz, 20 °C): δ 6.94 (ps. t, $^3J_{HH}$ = 7 Hz, 1H; p-$C_6H_3(CH_2P(CF_3)_2)_2$), 6.82 (ps. d, $^3J_{HH}$ = 7 Hz, 2H; m-$C_6H_3(CH_2P(CF_3)_2)_2$), 3.35 (br m, 4H; $C_6H_3(CH_2P(CF_3)_2)_2$), 2.07 (d, $^2J_{PH}$ = 5 Hz, 3H; $CH_3P(C_2F_5)_2$). $^{31}P\{^1H\}$ NMR (C_6D_6, 161.97 MHz, 20 °C): δ 67.3 (m, 2P; $P(CF_3)_2$), 37.1 (m, 1P; $MeP(C_2F_5)_2$). ^{19}F NMR (C_6D_6, 376.50 MHz, 20 °C): δ −56.2 (br m, 12F; PCF_3), −77.4 (s, 6F; $MeP(CF_2CF_3)_2$), ABX δ_A −114.7 ($^2J_{FF}$ = 294 Hz, $^2J_{FP}$ = 30 Hz, 2F; $(CH_3)P(CF_2CF_3)_2$), δ_B −116.5 ($^2J_{FF}$ = 294 Hz, $^2J_{FP}$ = 68 Hz, 2F; $(CH_3)P(CF_2CF_3)_2$).

$(^{CF_3}PCP)Ir(dfmp)_2$ (6). Complex **5** (20 mg, 0.021 mmol) was placed in an NMR tube and dissolved in 0.75 mL of C_6D_6. dfmp (39 μL, 62 mg, 0.218 mmol) was syringed into the NMR tube, whereupon the solution became pale yellow. After the solution stood undisturbed for 2 h, colorless crystals began to form. The reaction mixture was left undisturbed for a total of 20 h. Crystals suitable for single-crystal X-ray diffraction were obtained from the tube. Complex **6** is unstable in solution and is highly insoluble in C_6D_6. Attempts to isolate **6** failed, as the solid converts to **5** under vacuum and under an N_2 atmosphere.

$(^{CF_3}PCP)Ir(nbe)$ (7). $(^{CF_3}PCP)Ir(C_2H_4)(H)Cl$ (0.194 g, 0.278 mmol), Et_3N (0.50 mL, 0.363 g, 3.594 mmol), and norbornene (0.500 g, 5.311 mmol) were dissolved in benzene. One atmosphere of C_2H_4 was introduced, and the reaction mixture was stirred at ambient temperature for 20 h. Precipitation of $Et_3NH^+Cl^-$ was observed, and ^{31}P and ^{19}F NMR showed the major species in solution to be **4**. The ammonium salt was filtered away, and the volatiles were removed, giving an orange oil. The oil was dissolved in 15 mL of hexane and the solution filtered to remove a small amount of solid, and reduction to ca. 5 mL and cooling to −78 °C yielded the yellow-orange solid **7** (0.112 g, 55% yield). Crystals suitable for X-ray diffraction were grown by evaporation from a hexane solution. Anal. Calcd for $C_{19}H_{17}P_2F_{12}Ir$: C, 31.37; H, 2.36. Found: C, 30.99; H, 2.35. ^1H NMR (C_6D_6, 400.13 MHz, 20 °C): δ 7.03 (t, $^3J_{HH}$ = 8 Hz, 1H; p-$C_6H_3(CH_2P(CF_3)_2)_2$), 6.88 (d, $^3J_{HH}$ = 8 Hz, 2H; m-$C_6H_3(CH_2P(CF_3)_2)_2$), 4.11 (t, $^3J_{PH}$ = 5 Hz, 2H; nbe vinylic CH), 3.38 (ps. t, J_{PH} = 4 Hz, 4H; $C_6H_3(CH_2P(CF_3)_2)_2$), 3.11 (s, 2H; nbe CH), 1.28 (d, $^2J_{HH}$ = 8 Hz, 2H; nbe CH_2CH_2), 0.96 (d, $^2J_{HH}$ = 8 Hz, 2H; nbe CH_2CH_2), 0.55 (d, $^2J_{HH}$ = 10 Hz, 1H; nbe $CHCH_2CH$), 0.24 (d, $^2J_{HH}$ = 10 Hz, 1H; nbe $CHCH_2CH$). ^{13}C NMR (C_6D_6, 100.61 MHz, 20 °C): δ 157.5 (m; C_{Ar}-$CH_2P(CF_3)_2$), 143.1 (t, $^2J_{CP}$ = 13 Hz; C_{Ar}-Ir), 124.3 (d, $^1J_{CH}$ = 162 Hz; p-$C_6H_3(CH_2P(CF_3)_2)$, 122.6 (dm, $^1J_{CH}$ = 159 Hz; m-$C_6H_3(CH_2P(CF_3)_2)$, 70.1 (d, $^1J_{CH}$ = 171 Hz; nbe vinylic CH), 45.4 (d, $^1J_{CH}$ = 148 Hz; nbe CH), 42.7 (t, $^1J_{CH}$ = 134 Hz; nbe $CHCH_2CH$), 38.5 (tm, $^1J_{CH}$ = 136 Hz; $CH_2P(CF_3)_2$), 28.4 (t, $^1J_{CH}$ = 135 Hz; nbe CH_2CH_2). $^{31}P\{^1H\}$ NMR (C_6D_6, 161.97 MHz, 20 °C): δ 66.0 (m). ^{19}F NMR (C_6D_6, 376.50 MHz, 20 °C): δ −57.8 (m, 12F; PCF_3).

$(^{CF_3}PCP)Ir(coe)$ (8). Compound **8** was prepared from 0.300 g (0.430 mmol) of $(^{CF_3}PCP)Ir(C_2H_4)(H)Cl$ and 0.50 mL of Et_3N (3.594 mmol) analogously to **7**, except that cyclooctene (0.5 mL, 0.423 g, 3.839 mmol) was used instead of norbornene. After the reaction solution was filtered to remove $Et_3NH^+Cl^-$ and dissolved in hexanes, a small amount of solid was removed by filtration and a viscous red oil was obtained. Further purification was not possible, and the product was judged to be about +90% pure by NMR. ^1H NMR (C_6D_6, 400.13 MHz, 20 °C): δ 7.01 (t, $^3J_{HH}$ = 8 Hz, 1H; p-$C_6H_3(CH_2P(CF_3)_2)_2$), 6.89 (d, $^3J_{HH}$ = 8 Hz, 2H; m-$C_6H_3(CH_2P(CF_3)_2)_2$), 5.03 (br s, 2H; coe vinylic CH), 3.36 (ps. t, $^3J_{PH}$ = 4 Hz, 4H; $C_6H_3(CH_2P(CF_3)_2)_2$), 2.51 (m, 2H; coe

CH_2), 2.18 (m, 2H; coe CH_2), 1.52 (m, 4H; coe CH_2), 1.33 (m, 4H; coe CH_2). ^{13}C NMR (C_6D_6, 100.61 MHz, 20 °C): δ 146.1 (t, $^2J_{CP}$ = 10 Hz; C_{Ar}-Ir), 122.5 (dm, $^1J_{CH}$ = 158 Hz; *m*-$C_6H_3(CH_2P(CF_3)_2)$), 79.6 (d, $^1J_{CH}$ = 155 Hz; coe vinylic *C*H), 38.2 (tm, $^1J_{CH}$ = 136 Hz; $C_6H_3(CH_2P(CF_3)_2)_2)$), 33.2 (t, $^1J_{CH}$ = 127 Hz; coe CH_2), 32.6 (t, $^1J_{CH}$ = 127 Hz; coe CH_2), 26.2 (t, $^1J_{CH}$ = 122 Hz; coe CH_2). ^{31}P{^{1}H} NMR (C_6D_6, 161.97 MHz, 20 °C): δ 60.8 (m). ^{19}F NMR (C_6D_6, 376.50 MHz, 20 °C): δ −56.1 (br s, 12F; PCF_3).

(^{CF_3}PCP)Ir(H)$Cl_2^-HNEt_3^+$ (9). The reaction between (^{CF_3}PCP)Ir(C_2H_4)(H)Cl (0.277 g, 0.396 mmol) and Et_3N (0.50 μL, 3.6 mmol) was carried out in the absence of added ethylene using 10 mL of 95% 1,1-dimethyl-3-butene as the solvent. After 5 min, a precipitate of **9** began to form. The reaction mixture was stirred at ambient temperature for 1 h, and the brick red precipitate was collected via filtration (0.138 g, 86% based on 50% theoretical yield). In a separate NMR experiment, agitating a 1/1 mixture of (^{CF_3}PCP)Ir(C_2H_4)(H)Cl and $HNEt_3^+Cl^-$ in benzene at 20 °C for 20 min resulted in the quantitative formation of **9**. Crystals suitable for X-ray diffraction were obtained by slow evaporation from a benzene solution. Anal. Calcd for $C_{18}H_{24}NP_2F_{12}Cl_2Ir$: C, 26.78; H, 3.00; N, 1.73. Found: C, 27.31; H, 2.90; N, 1.67. ^{1}H NMR (C_6D_6, 400.13 MHz, 20 °C): δ 8.73 (br s, 1H; $HNEt_3^+$), 6.74 (m, 3H; $C_6H_3(CH_2P(CF_3)_2)_2$), 3.80 (br d, $^2J_{HH}$ = 17 Hz, 2H; $C_6H_3(CH_2P(CF_3)_2)_2$), 3.28 (br d, $^2J_{HH}$ = 17 Hz, 2H; $C_6H_3(CH_2P(CF_3)_2)_2$), 2.31 (q, $^3J_{HH}$ = 7 Hz, 6H; $HN(CH_2CH_3)_3^+$), 0.62 (m, 9H; $HN(CH_2CH_3)_3^+$), −19.18 (t, $^2J_{HP}$ = 17 Hz, 1H; IrH). ^{31}P{^{1}H} NMR (C_6D_6, 161.97 MHz, 20 °C): δ 53.1 (m). ^{19}F NMR (C_6D_6, 376.50 MHz, 20 °C): δ −54.9 (m, 6F; PCF_3), −60.5 (m, 6F; PCF_3).

(^{CF_3}PCP)Ir(nbd) (10). (^{CF_3}PCP)Ir(C_2H_2)(H)Cl (0.250 g, 0.358 mmol), Et_3N (150 μL, 0.109 g, 1.076 mmol), and nbd (0.25 mL, 0.276 g, 2.995 mmol) were dissolved in 15 mL of benzene. The reaction mixture was stirred at ambient temperature for 24 h, producing a pale yellow solution and a white $Et_3NH^+Cl^-$ precipitate. The salt was filtered away, and the volatiles were removed. The filtrate residue was dissolved in 15 mL of hexane, giving a small amount of solid which was filtered off and rinsed twice with 10 mL of hexane. The filtrate was cooled to −78 °C, which gave the product as a white solid that was collected via cold filtration (0.212 g, 81% yield). Anal. Calcd for $C_{19}H_{15}P_2F_{12}Ir$: C, 31.40; H, 2.08. Found: C, 31.77; H, 2.19. ^{1}H NMR (C_6D_6, 400.13 MHz, 20 °C): δ 6.70 (m, 3H; $C_6H_3(CH_2P(CF_3)_2)_2$), 4.28 (br m, 2H; nbd, uncoordinated vinylic CH), 3.68 (dd, $^2J_{HH}$ = 16 Hz, $^2J_{HP}$ = 12 Hz, 2H; $C_6H_3(CH_2P(CF_3)_2)_2$), 3.28 (d, $^2J_{HH}$ = 16 Hz, 2H; $C_6H_3(CH_2P(CF_3)_2)_2$), 3.26 (br s, 2H; nbd), 2.34 (m, 2H; nbd, coordinated vinylic CH), δ_A 0.37 and δ_B 0.31 (AB, $^2J_{HH}$ = 9 Hz, 2H; nbd CH_2). ^{13}C NMR (C_6D_6, 100.61 MHz, 20 °C): δ 146.8 (m; C_{Ar}-$CH_2P(CF_3)_2$), 139.7 (m; C_{Ar}-Ir), 124.7 (d, $^1J_{CH}$ = 161 Hz; *p*-$C_6H_3(CH_2P(CF_3)_2)$), 122.2 (dm, $^1J_{CH}$ = 149 Hz; *m*-$C_6H_3(CH_2P(CF_3)_2)$), 66.2 (t, $^1J_{CH}$ = 132 Hz; nbd $CHCH_2CH$), 60.8 (d, $^1J_{CH}$ = 180 Hz; nbd HC=CH), 45.4 (d, $^1J_{CH}$ = 150 Hz; nbd $CHCH_2CH$), 41.3 (td, $^1J_{CH}$ = 132 Hz, $^1J_{CP}$ = 38 Hz; $CH_2P(CF_3)_2$), 28.0 (t, $^1J_{CH}$ = 181 Hz, $^2J_{CP}$ = 20 Hz; nbd HC=CH). ^{31}P{^{1}H} NMR (C_6D_6, 161.97 MHz, 20 °C): δ 41.3 (m). ^{19}F NMR (C_6D_6, 376.50 MHz, 20 °C): δ −56.8 (d, $^2J_{FP}$ = 64 Hz, 6F; PCF_3), −61.2 (d, $^2J_{FP}$ = 67 Hz, 6F; PCF_3).

(^{CF_3}PCP)Ir(cod) (11). The procedure for the synthesis of **11** is the same as for **10**, except cod (0.25 mL, 0.221 g, 2.084 mmol) was used instead of nbd. Isolated yield: 0.244 g, (92%). Crystals suitable for X-ray diffraction were grown by diffusion of hexane into a saturated benzene solution. Anal. Calcd for $C_{19}H_{15}P_2F_{12}Ir$: C, 32.34; H, 2.58. Found: C, 32.66; H, 2.13. ^{1}H NMR (C_6D_6, 400.13 MHz, 20 °C): δ 6.73 (m, 3H; $C_6H_3(CH_2P(CF_3)_2)_2$), 4.87 (m, 2H; cod, noncoordinated vinylic CH), 3.58 (dd, $^2J_{HH}$ = 16 Hz, $^2J_{PH}$ = 12 Hz, 2H; $C_6H_3(CH_2P(CF_3)_2)_2$), 3.24 (d, $^2J_{PH}$ = 16 Hz, 2H; $C_6H_3(CH_2P(CF_3)_2)_2$), 2.50 (m, 2H; cod, coordinated vinylic CH), 2.28 (m, 2H; cod CH_2), 2.15 (m, 2H; cod CH_2), 1.95 (m, 2H; cod CH_2), 1.47 (m, 2H, cod CH_2). ^{13}C NMR (C_6D_6, 100.61 MHz, 20 °C): δ 147.0 (s; C_{Ar}-$CH_2P(CF_3)_2$), 140.3 (m; C_{Ar}-Ir), 124.8 (d, $^1J_{CH}$ = 160 Hz; *p*-$C_6H_3(CH_2P(CF_3)_2)$), 122.7 (dd, $^1J_{CH}$ = 162 Hz, $^3J_{CP}$ = 15 Hz; *m*-$C_6H_3(CH_2P(CF_3)_2)$), 80.6 (d, $^1J_{CH}$ = 162 Hz; cod HC=CH), 60.0 (dd, $^1J_{CH}$ = 157 Hz, $^2J_{CP}$ = 22 Hz; cod HC=CH), 40.4 (td, $^1J_{CH}$ = 136 Hz, $^1J_{CP}$ = 34 Hz; $CH_2P(CF_3)_2$), 34.7 (t, $^1J_{CH}$ = 126 Hz; cod CH_2CH_2), 29.0 (t, $^1J_{CH}$ = 126 Hz; cod CH_2CH_2). ^{31}P{^{1}H} NMR (C_6D_6, 161.97 MHz, 20 °C): δ 41.8 (m). ^{19}F NMR (C_6D_6, 376.50 MHz, 20 °C): δ −55.6 (d, $^2J_{FP}$ = 60 Hz, 6F; PCF_3), −59.9 (d, $^2J_{FP}$ = 60 Hz, 6F; PCF_3).

(^{CF_3}PCP)Ir(dfepe) (12). (^{CF_3}PCP)Ir(C_2H_4)(H)Cl (0.421 g, 0.603 mmol), Et_3N (0.50 mL, 3.594 mmol), and 1 atm of C_2H_4 were stirred overnight in 15 mL of toluene at room temperature to give **4** and a $HNEt_3^+Cl^-$ precipitate. The salt was filtered away under 1 atm of C_2H_4, and dfepe (283 μL, 0.840 mmol) was added to the filtrate. After the reaction mixture was stirred at ambient temperature for 16 h, a pale yellow solution with a pale yellow precipitate of **12** was produced. The volume was reduced to ca. 6 mL, and **12** was collected via filtration (0.454 g, 63% yield). Crystals suitable for X-ray diffraction were obtained by slow evaporation from a benzene solution. Anal. Calcd for $C_{22}H_{11}P_4F_{32}Ir$: C, 22.03; H, 0.92. Found: C, 21.89; H, 0.99. ^{1}H NMR ($CDCl_3$, 400.13 MHz, 20 °C): δ 7.11 (d, $^3J_{HH}$ = 7 Hz, 2H; *m*-$C_6H_3(CH_2P(CF_3)_2)_2$), 6.99 (t, $^3J_{HH}$ = 7 Hz, 1H; *m*-$C_6H_3(CH_2P(CF_3)_2)_2$), 4.05 (dd, $^2J_{HH}$ = 18 Hz, $^2J_{PH}$ = 11 Hz, 2H; $C_6H_3(CH_2P(CF_3)_2)_2$), 3.71 (d, $^2J_{HH}$ = 18 Hz, 2H; $C_6H_3(CH_2P(CF_3)_2)_2$), 2.62 (m, 2H; dfepe CH_2), 2.29 (m, 2H; dfepe CH_2). ^{31}P{^{1}H} NMR ($CDCl_3$, 161.97 MHz, 20 °C): δ 72.7 (m, 1P; $P(CF_3)_2$), 53–43 ppm (overlapping m, 3P; $P(CF_3)_2$ and dfepe). ^{19}F NMR ($CDCl_3$, 376.50 MHz, 20 °C): δ −54.3 (br s, 6F; PCF_3), −62.5 (d, $^2J_{FP}$ = 64 Hz, 6F; PCF_3), −76.0 (s, 6F; dfepe PCF_2CF_3), −76.1 (s, 6F; dfepe PCF_2CF_3), −101 to −109 (overlapping ABX multiplets, 8F; dfepe PCF_2CF_3).

(^{CF_3}PCP)Ir(PhCN)(C_2H_4) (13). (^{CF_3}PCP)Ir(PhCN)(H)Cl (0.400 g, 0.517 mmol), PhCN (0.53 mL, 0.533 g, 5.175 mmol), and Et_3N (0.720 mL, 0.523 g, 5.175 mmol) were dissolved in 15 mL of benzene. One atmosphere of C_2H_4 was introduced, and the reaction mixture was stirred at ambient temperature for 24 h. The $Et_3NH^+Cl^-$ precipitate was filtered away, and the volatiles were removed under vacuum. The residue was extracted with hexanes (∼45 °C, 25 mL), and the remaining solid was extracted with several portions of warm hexane. The filtrate volume was reduced to ca. 10 mL, and a pale orange solid was isolated and dried under vacuum (0.176 g, 44% yield). Crystals suitable for X-ray diffraction were obtained by diffusion of hexane into a saturated benzene solution. Anal. Calcd for $C_{21}H_{16}NP_2F_{12}Ir$: C, 32.99; H, 2.11; N, 1.83. Found: C, 32.88; H, 2.04; N, 1.58. ^{1}H NMR (C_6D_6, 400.13 MHz, 20 °C): δ 6.69 (m, 6H; $C_6H_3(CH_2P(CF_3)_2)_2$ and *o,p*-C_6H_5CN), 6.49 (ps t, $^3J_{HH}$ = 8 Hz, 2H; *m*-C_6H_5CN), 3.52 (m, 2H; $C_6H_3(CH_2P(CF_3)_2)_2$), 3.37 (m, 2H; $C_6H_3(CH_2P(CF_3)_2)_2$), 2.60 (br s, 2H; CH_2CH_2), 1.76 (br s, 2H; CH_2CH_2). ^{13}C NMR (C_6D_6, 100.61 MHz, 20 °C): δ 142.6 (s; C_{Ar}-$CH_2P(CF_3)_2$), 140.6 (m; C_{Ar}-Ir), 132.6 (dm, $^1J_{CH}$ = 163 Hz; C_6H_5CN), 131.9 (dt, $^1J_{CH}$ = 168 Hz, $^2J_{CH}$ = 6 Hz; C_6H_5CN), 128.4 (dm, $^1J_{CH}$ = 165 Hz; C_6H_5CN), 123.9 (d, $^1J_{CH}$ = 160 Hz; *p*-$C_6H_3(CH_2P(CF_3)_2)$), 122.4 (dm, $^1J_{CH}$ = 158 Hz; *m*-$C_6H_3(CH_2P(CF_3)_2)$), 119.3 (s; C_6H_5CN), 109.9 (d, J_{CH} = 9 Hz; *ipso*-C_6H_5CN), 38.2 (td, $^1J_{CH}$ = 134 Hz, $^1J_{CP}$ = 33 Hz; $CH_2P(CF_3)_2$), 32.4 (t, $^1J_{CH}$ = 157 Hz; Ir(C_2H_4)). ^{31}P{^{1}H} NMR (C_6D_6, 161.97 MHz, 20 °C): δ 50.5 (m). ^{19}F NMR (C_6D_6, 376.50 MHz, 20 °C): δ −56.8 (d, $^3J_{FP}$ = 60 Hz, 6F; PCF_3), −62.3 (d, $^3J_{FP}$ = 64 Hz, 6F; PCF_3).

(^{CF_3}PCP)Ir(CO)(CH_3)I (14). An NMR tube was charged with a ca. 50 mg sample of **1** (0.076 mmol), 0.5 mL of C_6D_6, and CH_3I (ca. 0.1 mL, 0.153 g, 1.011 mmol). Upon mixing the solution immediately changed from orange to colorless. The solution was transferred to a 5 mL glass vial, ca. 3.5 mL of hexanes was added, and the solution was slowly evaporated to give clear crystals suitable for single-crystal X-ray diffraction studies (0.052 g, 82% yield). Anal. Calcd for $C_{14}H_{10}P_2F_{12}OIIr$: C, 20.90; H, 1.25. Found: C, 21.16; H, 1.01. ^{1}H NMR (C_6D_6, 400.13 MHz, 20 °C): δ 6.75 (t, $^3J_{HH}$ = 7.6 Hz, 1H; p-$C_6H_3(CH_2P(CF_3)_2)_2$), 6.68 (d, $^3J_{HH}$ = 7.6 Hz, 2H; m-$C_6H_3(CH_2P(CF_3)_2)_2$), 3.95 (dt, $^2J_{HH}$ = 17 Hz, J_{PH} = 6 Hz, 2H; $C_6H_3(CH_2P(CF_3)_2)_2$), 3.43 (dt, $^2J_{HH}$ = 17 Hz, J_{PH} = 5 Hz, 2H; $C_6H_3(CH_2P(CF_3)_2)_2$), 0.50 (t, $^3J_{PH}$ = 6 Hz, 3H; Ir-CH_3). $^{31}P\{^1H\}$ NMR (C_6D_6, 161.97 MHz, 20 °C): δ 49.9 (m). ^{19}F NMR (C_6D_6, 376.50 MHz, 20 °C): δ −50.3 (m, 6F; PCF_3), −52.2 (m, 6F; PCF_3). IR (CH_2Cl_2, cm^{-1}): ν(CO) = 2082 cm^{-1}.

***trans*-(^{CF_3}PCP)Ir(CO)$(H)_2$ (15).** An NMR tube was charged with a ca. 15 mg sample of **1** (0.021 mmol) and 0.5 mL of C_6D_6. Hydrogen gas (1 atm) was introduced into the tube, and the solution changed from orange to colorless upon shaking. NMR spectra indicated the clean formation of the *trans*-dihydride **15**. ^1H NMR (C_6D_6, 400.13 MHz, 20 °C): δ 6.79 (t, $^3J_{HH}$ = 8 Hz, 1H; p-$C_6H_3(CH_2P(CF_3)_2)_2$), 6.59 (d, $^3J_{HH}$ = 8 Hz, 2H; m-$C_6H_3(CH_2P(CF_3)_2)_2$), 3.28 (m, 4H; $C_6H_3(CH_2P(CF_3)_2)_2$), −9.10 (t, $^2J_{HP}$ = 19.2 Hz, T_1 = 9.98 s, 2H; Ir-H). $^{31}P\{^1H\}$ NMR (C_6D_6, 161.97 MHz, 20 °C): δ 59.7 (m). ^{19}F NMR (C_6D_6, 376.50 MHz, 20 °C): δ −62.6 (br m, 12F; PCF_3). IR (CH_2Cl_2, cm^{-1}): ν(CO) 2068 cm^{-1}, ν(IrH) 2090 cm^{-1} (sh).

***fac,cis*-(^{CF_3}PCP)Ir(dfmp)$(H)_2$ (16).** An NMR tube was charged with a ca. 21 mg sample of **5** (0.021 mmol) and 0.5 mL of C_6D_6. Hydrogen gas (1 atm) was introduced into the tube, and the solution changed from orange to colorless upon shaking. NMR spectra indicated the clean formation of **16**. ^1H NMR (C_6D_6, 400.13 MHz, 20 °C): δ 6.85 (t, $^3J_{HH}$ = 7 Hz, 1H; p-$C_6H_3(CH_2P(CF_3)_2)_2$), 6.71 (d, $^3J_{HH}$ = 7 Hz, 2H; m-$C_6H_3(CH_2P(CF_3)_2)_2$), 3.73 (dd, $^2J_{HH}$ = 18 Hz, $^2J_{HP}$ = 15 Hz, 2H; $C_6H_3(CH_2P(CF_3)_2)_2$), 3.08 (d, $^2J_{HH}$ = 18 Hz, 2H; $C_6H_3(CH_2P(CF_3)_2)_2$), 1.88 (d, $^2J_{PH}$ = 7 Hz, 3H; $CH_3P(CF_2CF_3)_2$), −11.44 (AA′MXX′, $^2J_{HH}$ = 9 Hz, $^2J_{PH}$ = −161, 32, 19 Hz (to dfmp), $^2J_{PP}$ = 5 Hz ($^2J_{PP}$ between ^{CF_3}PCP and dfmp was not determined), T_1 = 1.60 s, 2H; Ir-H). $^{31}P\{^1H\}$ NMR (C_6D_6, 161.97 MHz, 20 °C): δ 38.2 (m, 2P; $P(CF_3)_2$), 19.7 (m, 1P; $MeP(C_2F_5)_2$). ^{19}F NMR (C_6D_6, 376.50 MHz, 20 °C): δ −56.1 (d, $^2J_{FP}$ = 56 Hz, 6F; PCF_3), −58.0 (d, $^2J_{FP}$ = 60 Hz, 6F; PCF_3), −74.6 (s, 6F; $MeP(CF_2CF_3)_2$), −110.1 (dd, $^2J_{FF}$ = 309 Hz, $^2J_{FP}$ = 45 Hz, 2F; $MeP(CF_2CF_3)_2$), −114.2 (dd, $^2J_{FF}$ = 305 Hz, $^2J_{FP}$ = 79 Hz, 2F; $MeP(CF_2CF_3)_2$).

***mer,trans*-(^{CF_3}PCP)Ir(dfmp)$(H)_2$ (17).** After the NMR tube prepared from **16** was allowed to sit for 24 h, ca. 10% was converted to **17**. ^1H NMR (C_6D_6, 400.13 MHz, 20 °C): δ 6.81 (t, $^3J_{HH}$ = 7 Hz, 1H; p-$C_6H_3(CH_2P(CF_3)_2)_2$), 6.66 (d, $^3J_{HH}$ = 8 Hz, 2H; m-$C_6H_3(CH_2P(CF_3)_2)_2$), 3.41 (br s, 4H; $C_6H_3(CH_2P(CF_3)_2)_2$), 2.02 (d, $^2J_{HP}$ = 7 Hz, 2H; $CH_3P(CF_2CF_3)_2$), −10.18 (br dt, $^2J_{HP}$ = 20 Hz, 2H; Ir-H). $^{31}P\{^1H\}$ NMR (C_6D_6, 161.97 MHz, 20 °C): δ 51.8 (m, 2P; $P(CF_3)_2$), 18.0 (m, 1P; $MeP(C_2F_5)_2$). ^{19}F NMR (C_6D_6, 376.50 MHz, 20 °C): δ −59.9 (ps. t, $^2J_{FP}$ = 38 Hz, 12F; PCF_3), −74.2 (s, 6F; $MeP(CF_2CF_3)_2$), −108.6 to −114.2 (overlapping ABX with **16**; $MeP(CF_2CF_3)_2$).

Variable-Temperature NMR Study of (^{CF_3}PCP)Ir(CO) + H_2. A 15 mg portion of (^{CF_3}PCP)Ir(CO) was dissolved in 0.5 mL of acetone-d_6 and cooled to −80 °C. Three atmospheres of H_2 was admitted, and after thorough mixing, the tube was placed in the NMR probe cooled to −60 °C. Spectral data for *fac,cis*-(^{CF_3}PCP)Ir(CO)$(H)_2$ (**18**): ^1H NMR (acetone-d_6, 400.13 MHz, −60 °C) δ 7.26 (d, $^3J_{HH}$ = 7 Hz, 2H; m-$C_6H_3(CH_2P(CF_3)_2)_2$), 7.05 (t, $^3J_{HH}$ = 7 Hz, 1H; p-$C_6H_3(CH_2P(CF_3)_2)_2$), 4.74 (dd, $^2J_{HH}$ = 16 Hz, $^2J_{HP}$ = 14 Hz, 2H; $C_6H_3(CH_2P(CF_3)_2)_2$), 4.20 (d, $^2J_{HP}$ = 16 Hz, 2H; $C_6H_3(CH_2P(CF_3)_2)_2$), −9.79 (AA′XX′, $^2J_{HP}$ = −157, 33 Hz, $^2J_{HH}$ = 12 Hz, $^2J_{PP}$ = 10 Hz, T_1 = 868 ms, 2H; Ir-H); $^{31}P\{^1H\}$ NMR (acetone-d_6, 161.97 MHz, −60 °C) δ 46.1 (m); ^{19}F NMR (acetone-d_6, 376.50 MHz, −60 °C) δ −59.9 (d, $^2J_{FP}$ = 68 Hz, 6F; PCF_3), −62.3 (d, $^2J_{FP}$ = 64 Hz, 6F; PCF_3). Spectral data for *mer,cis*-(^{CF_3}PCP)Ir(CO)$(H)_2$ (**19**): ^1H NMR (acetone-d_6, 400.13 MHz, −20 °C) δ 7.30 (d, $^3J_{HH}$ = 7 Hz, 2H; m-$C_6H_3(CH_2P(CF_3)_2)_2$), 7.08 (t, $^3J_{HH}$ = 7 Hz, H; p-$C_6H_3(CH_2P(CF_3)_2)_2$), 4.66 (m, 4H; $C_6H_3(CH_2P(CF_3)_2)_2$), −11.30 (t, $^2J_{HH}$ = 18 Hz, 1H; Ir-H), −11.72 (t, $^2J_{HH}$ = 16 Hz, T_1 = 2.79 s, 1H; Ir-H); $^{31}P\{^1H\}$ NMR (acetone-d_6, 161.97 MHz, −20 °C) δ 57.8 (m); ^{19}F NMR (acetone-d_6, 376.50 MHz, −20 °C) δ −62.8 (m, 6F; PCF_3), −65.0 (m, 6F; PCF_3).

Dynamic NMR Analysis. All examined fluxional systems (compounds **3**, **4**, **13**, and **18**) were modeled using iNMR.[31] Dynamic line shape fitting was applied to resonances in the intermediate exchange regime or at coalescence. Probe temperatures were not calibrated and were assumed to be ±2 °C.

X-ray Crystallography. The X-ray diffraction data for all complexes were measured at 150 K on a Bruker SMART APEX II CCD area detector system equipped with a graphite monochromator and a Mo Kα fine-focus sealed tube operated at 1.5 kW power (50 kV, 30 mA). Crystals were attached to either a Hampton Research cryoloop or a MiTeGen micromount using Paratone N oil. The detector was placed at a distance of 5.9 cm from the crystal during the data collection.

A series of narrow frames of data were collected with a scan width of 0.5° in ω or ϕ and an exposure time of 10 s per frame. The frames were integrated with the Bruker SAINT Software package[32] using a narrow-frame integration algorithm. The data were corrected for absorption effects by the multiscan method (SADABS). Crystallographic data collection parameters and refinement data are deposited as Supporting Information. The structures of **2**, **3**, **9**, **11**, and **13** were solved by direct methods, and the structures of **1**, **5−7**, **12**, **14**, and **16** were solved by Patterson methods using the Bruker SHELXTL (V. 6.10 or V. 6.14) software package. All non-hydrogen atoms were located in successive Fourier maps and refined anisotropically. Hydrogen atoms for complexes **7** and **12** were located on difference Fourier maps and refined isotropically. Two sets of anions and cations were present in the asymmetric unit of **9**; the hydride ligands were located and refined isotropically. Crystals of complex **9** contained two benzene molecules per asymmetric unit; one CF_3 group and one benzene molecule were partially disordered but were not modeled. Methyl hydrogens for complex **14** were located and refined isotropically; one CF_3 group was rotationally disordered and was modeled satisfactorily using a two-position model. The $P\bar{1}$ asymmetric unit of **16** consists of three independent *trans*-(^{CF_3}PCP)Ir(dfmp)$(H)_2$ molecules. Molecules centered on Ir(1) and Ir(3) are well-ordered, whereas two of the C_2F_5 groups associated with Ir(2) are disordered. Assignment of two sets of positions for the disordered atoms led to satisfactory refinement of the structure. All hydride ligand atoms were located in the Fourier maps and refined isotropically. The rest of the hydrogen atoms were placed in calculated positions and were refined isotropically. In the remaining structures (**1−3**, **5**, **6**, **11**, and **13**) all hydrogen atoms were placed in calculated positions.

Computational Details. All calculations were carried using Gaussian 09 Rev. A.02.[33] The density functional theory (DFT) B97-1 hybrid exchange-correlation functional was used for geometry optimization and frequencies.[34] The Dunning cc-pVDZ

---

[31] *iNMR, Version 3.6.3*; http://www.inmr.net.

[32] *APEX2 Software Suite, Version 2.2*; Bruker AXS Inc., Madison, WI, 2008.

[33] Frisch, M. J.; Trucks, G. W.; Schlegel, H. B.; Scuseria, G. E.; Robb, M. A.; Cheeseman, J. R.; Scalmani, G.; Barone, V.; Mennucci, B.; Petersson, G. A.; Nakatsuji, H.; Caricato, M.; Li, X.; Hratchian, H. P.; Izmaylov, A. F.; Bloino, J.; Zheng, G.; Sonnenberg, J. L.; Hada, M.; Ehara, M.; Toyota, K.; Fukuda, R.; Hasegawa, J.; Ishida, M.; Nakajima, T.; Honda, Y.; Kitao, O.; Nakai, H.; Vreven, T.; Montgomery, Jr., J. A.; Peralta, J. E.; Ogliaro, F.; Bearpark, M.; Heyd, J. J.; Brothers, E.; Kudin, K. N.; Staroverov, V. N.; Kobayashi, R.; Normand, J.; Raghavachari, K.; Rendell, A.; Burant, J. C.; Iyengar, S. S.; Tomasi, J.; Cossi, M.; Rega, N.; Millam, N. J.; Klene, M.; Knox, J. E.; Cross, J. B.; Bakken, V.; Adamo, C.; Jaramillo, J.; Gomperts, R.; Stratmann, R. E.; Yazyev, O.; Austin, A. J.; Cammi, R.; Pomelli, C.; Ochterski, J. W.; Martin, R. L.; Morokuma, K.; Zakrzewski, V. G.; Voth, G. A.; Salvador, P.; Dannenberg, J. J.; Dapprich, S.; Daniels, A. D.; Farkas, Ö.; Foresman, J. B.; Ortiz, J. V.; Cioslowski, J.; Fox, D. J. *Gaussian 09, Rev. A.02*; Gaussian, Inc., Wallingford, CT, 2009.

basis set was used for all main-group elements; the diffuse basis set AUG-cc-pVDZ was used for phosphorus.[35] Figgen et al. energy-consistent pseudopotentials and correlation-consistent basis set for iridium was used.[36] The geometry optimization for the bis-ethylene complex **4** was carried out without any symmetry constraints; the absence of any imaginary frequencies confirmed the optimized structure shown in Figure 8 as an energy minimum.

Acknowledgment. We thank The National Science Foundation (No. CHE-0457435) and DOE/EPSCoR (No. DE-FG02-08ER15979) for financial support.

Supporting Information Available: CIF files giving crystallographic data for complexes **1**−**3**, **5**−**7**, **9**, **11**−**14**, and **16** and tables giving DFT optimization details and coordinates. This material is available free of charge via the Internet at http://pubs.acs.org.

---

(34) Hamprecht, F. A.; Cohen, A. J.; Tozer, D. J.; Handy, N. C. *J. Chem. Phys.* **1998**, *109*, 6264–6271.

(35) Dunning, T. H., Jr. *J. Chem. Phys.* **1989**, *90*, 1007–1023.

(36) Figgen, D.; Peterson, K. A.; Dolg, M.; Stoll, H. *J. Chem. Phys.* **2009**, *130*, 164108/164101–164108/164112.